ANL-77-75

Lb. 2020

ANL-77-75

182
11/17/78

MASTER

HIGH-PERFORMANCE BATTERIES FOR STATIONARY ENERGY STORAGE AND ELECTRIC-VEHICLE PROPULSION

Progress Report for the Period July—September 1977

U of C-AUA-USERDA

ARGONNE NATIONAL LABORATORY, ARGONNE, ILLINOIS

Prepared for the U. S. ENERGY RESEARCH AND DEVELOPMENT ADMINISTRATION under Contract W-31-109-Eng-38

DISCLAIMER

Printed in the United States of America
Available from
National Technical Information Service
U. S. Department of Commerce
5285 Port Royal Road
Springfield, Virginia 22161
Price: Printed Copy $6.00; Microfiche $3.00

Distribution Category:
Energy Storage—Electrochemical
(UC-94c)

ANL-77-75

Argonne National Laboratory
9700 South Cass Avenue
Argonne, Illinois 60439

HIGH-PERFORMANCE BATTERIES FOR STATIONARY ENERGY STORAGE AND ELECTRIC-VEHICLE PROPULSION

Progress Report for the Period
July—September 1977

P. A. Nelson	Director, Energy Storage
N. P. Yao	Associate Director, Energy Storage
R. K. Steunenberg	Manager, Lithium/Metal Sulfide Battery Program
A. A. Chilenskas	Manager, Battery Commercialization
E. C. Gay	Section Manager, Battery Engineering
J. E. Battles	Group Leader, Materials Development
F. Hornstra	Group Leader, Battery Charging Systems
W. E. Miller	Group Leader, Industrial Cell and Battery Testing
M. F. Roche	Group Leader, Cell Chemistry
H. Shimotake	Group Leader, Cell Development and Engineering

January 1978

Previous Reports in this Series

ANL-76-98	July—September 1976
ANL-77-17	October—December 1976
ANL-77-35	January—March 1977
ANL-77-68	April—June 1977

PREFACE

The program on high-temperature secondary batteries at Argonne National Laboratory consists of an in-house research and development effort and subcontracted work by industrial laboratories. The work at Argonne is carried out primarily in the Chemical Engineering Division, with assistance on specific problems being given by the Materials Science Division and, from time to time, by other Argonne divisions. The individual efforts of many scientists, engineers, and technicians are essential to the success of the program, and recognition of these efforts is reflected by the individual contributions cited throughout the report.

TABLE OF CONTENTS

TABLE OF CONTENTS (contd)

LIST OF FIGURES

LIST OF TABLES

HIGH-PERFORMANCE BATTERIES FOR STATIONARY ENERGY STORAGE AND ELECTRIC-VEHICLE PROPULSION

Progress Report for the Period
July—September 1977

ABSTRACT

This report describes the research, development, and management activities of the program at Argonne National Laboratory (ANL) on lithium/metal sulfide batteries during the period July-September 1977. These batteries are being developed for electric-vehicle propulsion and stationary energy storage. The present cells, which operate at 400-500°C, are of a vertically oriented, prismatic design with a central positive electrode of FeS or FeS_2, two facing negative electrodes of lithium-aluminum alloy, and an electrolyte of molten LiCl-KCl.

A major objective of this program is to transfer the technology to industry as it is developed, with the ultimate goal of a competitive, self-sustaining industry for the commercial production of lithium/metal sulfide batteries. Technology transfer is being implemented by several means, including the assignment of industrial participants to ANL for various periods of time and the subcontracting of development and fabrication work on cells, cell components, and battery testing equipment to industrial firms.

Testing and evaluation of industrially fabricated cells is continuing. These tests provide information on the effects of design modifications and alternative materials for cells. During this period, plans were laid for the construction of a 100-cell test facility, and a prototype 100-A cell/battery cycler was designed and built by the ANL Electronics Division. Improved electrode and cell designs are being developed and tested at ANL, and the more promising designs are incorporated into the industrially fabricated cells. Among the concepts receiving attention are carbon-bonded positive electrodes, pellet-grid electrodes, alternative materials for positive electrodes, additives to extend electrode lifetime, and alternative electrode separators.

Materials development efforts include the development of improved electrical feedthroughs, investigations of various types of electrode separators, corrosion and wettability studies of materials, and post-test examinations of cells. Cell chemistry studies are concerned with phases formed in FeS_2 electrodes, sulfur vaporization rates for FeS_2 and NiS_2, and cyclic voltammetry measurements of metal sulfide electrodes. Titanium disulfide positive electrodes as well as liquid lithium negative electrodes are also being investigated. In studies of advanced battery systems, the use of calcium and magnesium alloys for the negative electrode is being investigated.

SUMMARY

Commercial Development

To achieve successful commercialization of the lithium/metal sulfide battery, industry must be convinced that this battery is: technically feasible, marketable, and capable of meeting governmental requirements (with respect to safety, environment, etc.). A paper is being written on these three factors. In this paper, a schedule for the commercialization of the lithium/metal sulfide battery is developed.

A preliminary safety assessment by Budd Co. was conducted on the lithium/metal sulfide battery for an electric vehicle. These preliminary results indicate that the engineering of a safe vehicle powered by this type of battery may be less difficult than originally believed.

Industrial Contracts

Atomics International (a division of Rockwell International) is conducting a general research and development program in addition to design studies on the stationary energy storage battery. Catalyst Research Corp., Eagle-Picher Industries, Inc., and Gould Inc. are involved primarily with the development and fabrication of cells that are tested either at ANL or in their own laboratories.

Lead-acid batteries were obtained for a Renault electric vehicle, and the vehicle is now operational. Blake Electronics of Milwaukee was contracted to build a battery charger similar to that used in the Sears XDH-1 electric vehicle for use in the Renault.

Industrial Cell and Battery Testing

Cells incorporating modifications from baseline FeS and FeS_2 cells were fabricated by Eagle-Picher Industries, Inc., and tested at ANL. A group of FeS cells with thinner and denser positive electrodes than those of baseline cells gave the highest specific energy of any contractor-produced FeS cell--50 W-hr/kg at the 4-hr rate. Eagle-Picher FeS_2 cells with an improved version of the honeycomb current collector have shown the highest performance of any contractor-produced cell--80 W-hr/kg at the 4.5-hr rate. This improved design includes a flexible connection between the positive terminal rod and the current collector which eliminates stresses on the molybdenum weld. With minor mechanical changes to reduce the cell weight, the specific energy is expected to increase to 90 W-hr/kg at the 4-hr rate. Eagle-Picher is currently fabricating cells with variations on this cell design. Eagle-Picher FeS_2 cells with thinner and denser positive electrodes and no ZrO_2 fabric retainer for the negative electrode have also exhibited good performance, 70-75 W-hr/kg at the 4-hr rate; however, performance was lower than expected. The cause of the lower-than-expected specific energies was attributed to the use of lower electrolyte volume fractions in the positive electrodes of those cells.

The FeS_2 baseline cell, EP-2B8, was used to test the long-term effect of air on an operating cell. Testing of this cell, which was wrapped in Kaowool and operated in air, was voluntarily terminated after 378 days and 533 cycles. This cell demonstrated that operation in an air environment over a long

period of time can be accomplished without deleterious effects on cell performance. The FeS cell, EP-I-3-C-2, was used to compare a current-limited, constant-voltage (CLCV) charge with a constant-current charge. These tests suggested that CLCV charging does not significantly increase performance but does reduce charge time.

Testing of two FeS cells connected in series (Battery B7-S) has continued at the 10- and 5-hr rates, with and without equalization. This battery has operated for more than 377 days and 756 cycles. Equalization charging appears to have only marginal benefits. A five-cell battery (B12-S) was shut down after 34 cycles because of low voltage, and the five cells were placed in a test chamber and cycled individually. During cycling, one of the cells did not charge above 1.8 V. The three remaining cells were then connected in series, and placed in an insulated case. The individual cell resistances of this three-cell battery (B13-S) are relatively high (12 mΩ); this is reflected in the battery performance at high current rates.

Procurement of power supplies and the data-acquisition and computer-control system for a facility for testing 30-60 kW-hr batteries has been initiated. Plans are also in progress to build a 100-cell test facility. This facility will be used to determine product and performance reliability prior to the procurement of large numbers of cells for the electric-vehicle battery.

A prototype 100-A cell/battery cycler was designed and constructed by the ANL Electronics Division, and has been undergoing check-out. Various computer configurations and systems were reviewed and recommendations made.

A computer analysis of two different types of chargers, namely, a charger supplied with the Renault electric vehicle and a charger used on the Sears XDH-1 electric vehicle, was conducted to explore the behavior of these chargers under various charging conditions.

Cell Development and Engineering

One of the common reasons for cell failure is short circuits caused by extrusion of active material from the positive electrode. To prevent this from occurring, a Hastelloy B screen was added to the FeS_2 electrode of Cell R-30. Excellent utilization was achieved by this cell; however, the cell developed a short circuit after 48 days of operation.

The substitution of nickel sulfide for FeS_2 as the active material in the positive electrode is being explored. Two uncharged NiS_2 cells, R-31 and R-32, have been operated and tested. Carbon powder that had been heated previously to 1000°C was added to the positive electrode of Cell R-32. Both cells showed excellent coulombic efficiencies; however, the resistance of Cell R-32 was much lower than that of R-31.

A charged FeS_2 cell, M-4, was built with a BN felt spearator/retainer. The positive electrode consisted of a hot-pressed mixture of FeS_2, NiS, Mo, and Fe. After 27 cycles, the cell developed a short circuit, and operation was temporarily terminated. The cell was then reconstructed with a Y_2O_3 felt separator and restarted. Low resistance (3 mΩ) with high performance is being achieved by this rebuilt cell.

Operation of a carbon-bonded cell with a Y_2O_3 felt separator/retainer, Cell KK-11, was voluntarily terminated after 120 days and 223 cycles. Post-test examination showed that the amount of Li_2S in the separator was equivalent to that of a similar cell (M-3) which operated for a much shorter time (223 *vs.* 90 cycles). Experiments on small-scale cells indicated that cells with carbon powder previously treated at high temperatures (>1000°C) added to the positive electrode had about the same performance as cells with carbon-bonded positive electrodes.

An FeS_2 pellet cell has been constructed with a new pellet-grid design. This design has the desirable features of (1) alleviating the stress on the grid-to-current lead connection and (2) utilizing approximately 60% less molybdenum than is used in the current collector of the Eagle-Picher Type 2B baseline cell. Studies on small-scale cells indicated that adding molybdenum, either as powdered metal or as MoS_2, to the positive electrode greatly reduces electrode expansion during cycling. Construction of pellet cells using molybdenum additive is planned.

Investigation is continuing on the addition of a third metal to the negative electrode in FeS cells. Cell FM-4, in which zinc was added to the negative electrode, has operated for 70 cycles and 40 days without a significant improvement in performance over that of a cell with no additive. Of the negative electrode additives tested to date, tin enhanced cell capacity the most. An FeS_2 cell was built and operated with tin as an additive in the negative electrode; this additive did not stabilize cell capacity.

Three engineering-scale FeS_2 cells with ceramic powder separators were operated. Two of these cells had Y_2O_3 powder separators and the other had a MgO powder separator. Although these cells did not operate for more than 57 days, they produced high coulombic efficiencies and low internal resistances.

Materials Development

The ANL mechanical feedthrough has been redesigned. This new design utilizes a snap retainer ring, instead of a threaded nut or crimp, to close the seal. This new feedthrough is easy to assemble, lightweight, small, and inexpensive. Development work on brazed feedthroughs is temporarily inactive pending further evaluation of several developmental proposals from outside ANL.

Efforts are continuing on the evaluation of candidates for electrode separators (such as felts, papers, and powders) in small-scale, prismatic cells. Two test cells, one using BN felt and the other MgO powder as separator material, were operated for over 195 and 67 cycles, respectively. The preliminary results indicate that the percent utilization of the two cells is approximately the same at low current densities (about 80% at 20 mA/cm^2 and 60% at 40 mA/cm^2). However, at larger current densities, the utilization of the MgO-powder cell dropped off rather drastically compared to the BN-felt cell.

Out-of-cell compatibility tests were carried out to evaluate CaF_2 as a separator material. The results show that CaF_2 is not compatible with the cell environment.

A study of creep behavior has been initiated for various powder separator and electrode-separator systems. The coefficient of thermal expansion and the creep rate were determined for a compacted MgO powder saturated with eutectic salt.

Porous Y_2O_3 separators have been fabricated by conventional pressing-and-sintering procedures into rectangular shapes for in-cell testing. These separators have densities of 25 to 44% TD (theoretical density), and are as thin as 1.5 mm. Porous separators have also been prepared by casting Y_2O_3 plaster formulations into molds. This technique has yielded a specimen with a 25% TD. The procedures for forming, drying, and firing porous Y_2O_3 bodies are being refined; the best techniques will be used in fabricating separators for in-cell testing.

Further investigations into the reaction between aluminum and other metallic components of the negative electrode were made. Static immersion tests were carried out on unalloyed aluminum and low-carbon steel in LiCl-KCl eutectic obtained from Anderson Physics Laboratory and from Lithcoa Co. The tests confirmed the dependence of the iron-aluminum reaction rate on the pH of the salt. Other tests showed that the negative electrode must be depleted of lithium before this reaction can occur.

Electrolyte penetration tests have been completed on a series of rigid, porous Y_2O_3 separators. Sintered Y_2O_3 foams and powders exhibited easy-to-penetrate behavior.

A BN felt separator material (3 mm thick) has undergone wettability testing. The felt exhibited difficult-to-penetrate behavior. A procedure is suggested for out-of-cell infiltration of the felt with electrolyte. Various pretreatment processes were also tested as means of improving separator wettability. The only successful treatment found to date is immersion of the separator in molten $LiAlCl_4$ before cell assembly.

A quadrupole mass spectrometer for cell degassing studies has been tested, and found to be in need of repair. Sampling flasks have been fabricated and will be used shortly for analyses of the helium glovebox atmosphere.

Post-test examinations were continued on vertical, prismatic cells produced by ANL and by industrial contractors. Small-scale laboratory cells were also examined. The results of these post-test examinations are presented. These examinations showed a large amount of Li_2S in the separators of all FeS_2 cells except those cells in which nickel and/or Hastelloy B, rather than molybdenum, were used for current collectors in the positive electrode. This unusual behavior was confirmed by cells 2B-Fe-1 and 2B-Ni-1, which used sacrificial screens of iron and nickel on the faces of the positive electrodes. The amount of Li_2S observed in the separators of these two cells was much less than that observed in typical FeS_2 cells. Chemical analysis showed that the sulfur content in the separator of cell 2B-Fe-1 was 1.01 wt % and 2B-Ni-1 was 3.59 wt %. Separators from typical FeS_2 cells contain 6 to 10 wt % sulfur.

From the postoperative examinations, data have been obtained on the in-cell corrosion rate for the current collectors of FeS and FeS_2 cells. The corrosion rate in a negative electrode for the reaction of aluminum with low carbon steel ranged from 25 to 85 μm/yr penetration. In FeS positive electrodes, the

corrosion rate for the low-carbon steel was 50-125 μm/yr penetration. Molybdenum current collectors in FeS_2 positive electrodes showed only minor evidence of sulfide attack, with corrosion rates of 2 to 4 μm/yr.

Cell Chemistry

Studies were continued to determine the phases present during discharge of FeS_2 electrodes. One of the intermediate phases formed (designated Z phase) was found to have the composition $Li_3Fe_2S_4$. The composition of another phase (designated W phase) which exists in equilibrium with $Fe_{1-x}S$ in operating cells has not yet been determined.

Sulfur vaporization rates were measured at 527°C for FeS_2 and NiS_2 in either LiCl-KCl or LiCl-KCl plus Li_2S. The sulfur losses from NiS_2 in electrolyte were about a factor of three higher than losses from FeS_2. Vaporization rates are much higher for both sulfides after Li_2S additions, and the rates for both sulfides after Li_2S addition are about the same.

Slow-scan cyclic voltammetry data showed that NiS_2 has better electrochemical reversibility than FeS_2. Good reversibility was also observed for equimolar mixtures of NiS_2 and FeS_2. Electroreversibility was found to improve with increasing atomic number in the transition metal triad: Fe, Co, Ni.

Cell tests and cyclic voltammetry studies showed that the reaction,

$$FeS_2 + 3Li \rightleftarrows Li_3Fe_2S_4$$

is reversible. The electrochemical irreversibility of FeS_2 was identified as resulting from compounds present between 37.5 and 50% utilization of the theoretical capacity.

Tests of NiS_2 electrodes containing graphite, CoS_2, or molybdenum indicated that graphite is a better additive for this electrode than CoS_2 or molybdenum.

In small-scale LiAl/TiS_2 cells, the power capabilities of TiS_2 electrodes were similar to those of FeS_2 electrodes. Cells in which the positive electrode consisted of titanium sulfide compounds containing chromium, molybdenum, or copper have been operated. These cells did not appear to offer any advantages over cells with TiS_2 alone in the positive electrode.

A liquid lithium/FeS cell with a theoretical capacity of 70 A-hr achieved a specific energy of over 70 W-hr/kg, but developed a short circuit after 11 cycles. The short circuit was traced to swelling of the positive electrode. To prevent this swelling, a modular design for the positive electrode was developed.

Advanced Battery Research

Tests of nickel disulfide and iron-titanium sulfide electrodes were conducted in small-scale calcium cells. Utilizations of about 70% were achieved at current densities of 20 mA/cm^2. An engineering-scale Mg_2Si/Ni-CaS (uncharged) cell (theoretical capacity, 90 A-hr) was operated for 76 cycles. The coulombic

efficiency was satisfactory, but the utilization was only 33%. A reference electrode in the cell indicated that the positive electrode limited cell performance.

Tests of Mg_2Cu, NiS, NiS_2, and Mg_2Al_3 electrodes were conducted in small-scale magnesium cells. None of the electrodes demonstrated a performance that would justify scale-up of the magnesium cell at this time.

I. INTRODUCTION

Lithium/metal sulfide batteries are being developed at Argonne National Laboratory (ANL) for use as (1) power sources for electric vehicles, and (2) stationary energy storage devices for load-leveling on electric utility systems and storage of electrical energy produced by solar, wind, or other sources. The performance and lifetime goals that are projected for prototypes of electric vehicle and stationary energy storage batteries in 1985 are presented in Table I-1. Future revisions of these goals may be appropriate as the requirements of these two applications are defined more specifically through systems design studies.

The enactment of the Electric and Hybrid Vehicle Research and Development Act of 1976, Public Law 94-413, has resulted in an increased emphasis on the development of electric vehicle batteries of all types. In the case of lithium-aluminum/metal sulfide batteries, the present plans call for the development of a series of batteries--designated Mark I, II, and III--each of which has somewhat different objectives. The primary purpose of the Mark I battery is to establish the technical feasibility of the lithium-aluminum (or lithium-silicon)/ metal sulfide batteries for electric vehicle propulsion and to resolve any interfacing problems between this type of battery and a vehicle. The first tests will be conducted with an electric van in 1979. The Mark II batteries will be used to develop designs and materials that will decrease manufacturing costs, and to develop pilot-scale manufacturing techniques. The Mark II batteries are expected to have higher performance than the Mark I series. The Mark III battery is planned as a prototype for demonstration and evaluation in an electric passenger automobile in 1983. Program goals for the Mark I, II, and III batteries are listed in Table I-2.

Table I-1. Performance Goals for Lithium/Metal Sulfide Batteries

Battery Goals	Electric Vehicle Propulsion	Stationary Energy Storage
Power		
Peak	60 kW	25 MW
Sustained Discharge	25 kW	10 MW
Energy Output	45 kW-hr	100 MW-hr
Specific Energy,[a] W-hr/kg	180	60-150
Discharge Time, hr	4	5-10
Charge Time, hr	5-8	10
Cycle Life	1000	3000
Cost of Cells, $/kW-hr	35	20

[a]Includes cell weight only; the insulation and supporting structure is about 15 to 20% of the total weight for the electric vehicle battery.

Table I-2. Program Goals for the Mark I, II, and III Electric-Vehicle Batteries

	Mark I	Mark II	Mark III
Specific Energy, W-hr/kg			
Cell (average)	100	125	160
Battery	75	100	130
Energy Density, W-hr/liter			
Cell (average)	320	400	525
Battery	100	200	300
Peak Power, W/kg			
Cell (average)	100	125	200
Battery	75	100	160
Jacket Heat Loss, W	200	150	125
Lifetime			
Deep Discharges	400	500	1,000
Demonstration Target Date	1979	1981	1983

Late in August 1977, a decision was made to proceed with the procurement of the first Mark I battery, which is designated Mark IA. The Mark IA battery cells will have lithium-aluminum or lithium-silicon negative electrodes and FeS positive electrodes. Although a higher specific energy and specific power could be achieved with FeS_2 positive electrodes, FeS has been chosen because it is considered to be more reliable at the present time and because iron rather than molybdenum current collectors can be used. The Mark IA battery probably will consist of two units, each having a capacity of 20 kW-hr, a weight of about 340 kg, and a volume of approximately 200 liters. The battery will be designed to operate between 400 and 500°C, with a maximum total heat loss of 400 W. A request for proposals for the design, development, and fabrication of the Mark IA battery has been prepared, and will be issued shortly.

For the stationary energy storage battery, assessment studies have indicated that batteries having a life of 8 to 12 years and a capital cost of about $20 to $30/kW-hr would be competitive with alternative methods of storing energy or producing supplemental power during peak demand periods. Although these applications require long lifetime and low cost, the specific-energy and specific-power requirements for the cells are relatively modest. The cells currently under development for stationary energy storage batteries have lithium-aluminum or lithium-silicon negative electrodes and FeS positive electrodes.

Both ANL and the Atomics International Division of Rockwell International* have developed conceptual designs for cells and modules for stationary energy storage batteries that will eventually be tested in the Battery Energy Storage Test (BEST) Facility. A common conceptual design for a battery module based

*Under contract with ANL.

on these two designs will be developed as a cooperative effort between ANL and Atomics International, and this module will serve as a basis for a design of a utility storage plant with a 100 MW-hr capacity. Following this effort, component and subsystem testing in a mock-up facility is anticipated.

The lithium/metal sulfide battery program consists of an in-house research and development effort at ANL and subcontracts with several industrial firms. The major industrial subcontractors are Atomics International, Carborundum Co., Catalyst Research Corp., Eagle-Picher Industries, Inc., and Gould Inc. The ANL effort includes cell chemistry studies, materials development and evaluation, cell and battery development, industrial cell and battery testing, and commercialization studies. Preparations are also being made for in-vehicle tests of the Mark IA battery. Another small effort at ANL is directed toward the development of advanced battery systems that use low-cost, abundant materials.

Table I-3 shows the highest performance and lifetime achieved by the experimental and industrial contractors' cells operated during this quarter. (For a more detailed description of these cells, see Appendix A.) Cycle life data for all of the FeS and FeS_2 cells that were operated from October 1976 through September 1977 are presented in Fig. I-1. A total of 69 cells were cycled during this period.

Table I-3. Highest Cell Performance During this Quarter

Cell Type and Designation	Specific Energy, W-hr/kg	Specific Power, W/kg	Cycles
FeS			
1B4	60 (10)[a]	–	>789
I-3-B-2	60 (10)	32	>43
FeS_2			
I-6-B-1	67 (4)	52	>99
I-7-3	75 (4)	65	>55
M-4	104 (9)	145 (100% charged)	>36
	89 (4.5)	85 (50% discharged)	
	70 (2)	63 (25% discharged)	

[a]Number in parentheses indicates discharge rate in hours.

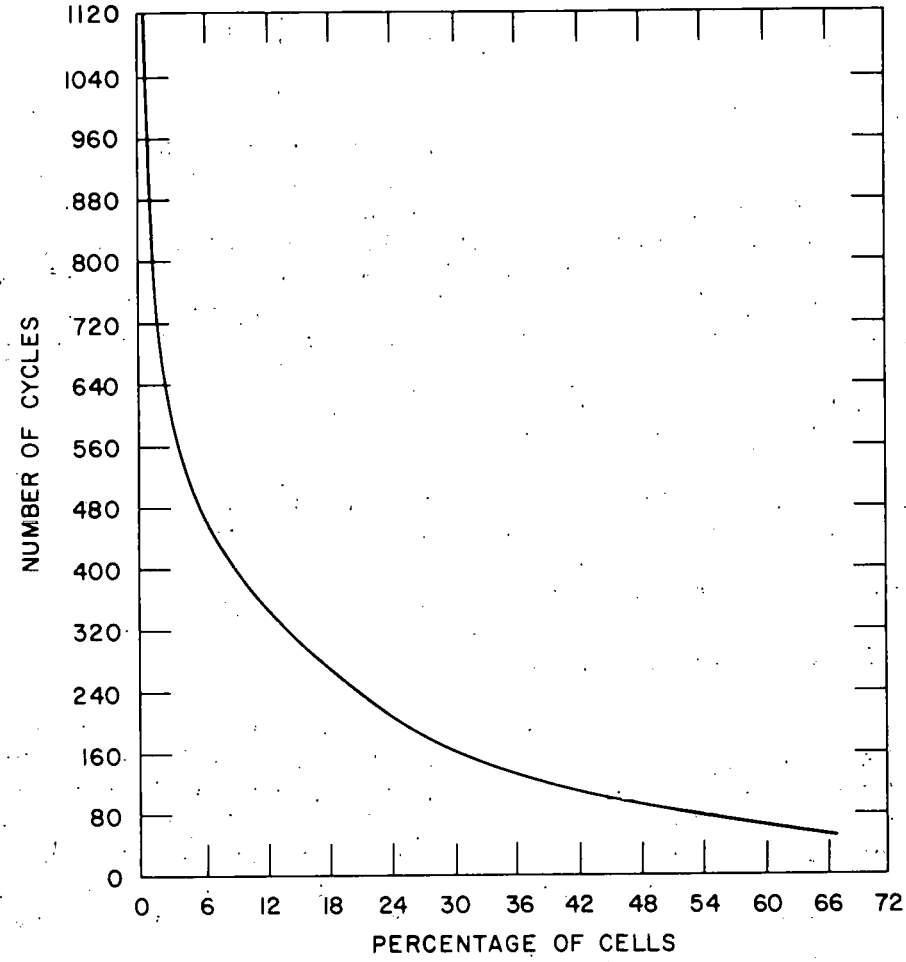

Fig. I-1. Number of Cycles *vs.* Percentage of Cells (FeS and FeS_2 cells operated over the previous year)

II. COMMERCIAL DEVELOPMENT
(A. A. Chilenskas)

The objective of the commercialization effort is to develop, with a minimum of federal support, a competitive self-sustaining industry capable of producing a supply of lithium/metal sulfide batteries that meets national needs. Commercialization planning has been undertaken to establish realistic technical and economic goals in meeting this objective. Important elements in our commercial development plan are the following: (1) materials and production costs for cells and assembled batteries, (2) marketing analyses, (3) manufacturing plans, and (4) analyses of competing systems and technologies.

A. Commercialization Studies
(A. A. Chilenskas, W. H. Towle*)

To achieve successful commercialization of the lithium/metal sulfide battery, industry must be convinced that this battery is:

1. Technically feasible
2. Marketable
3. Capable of meeting governmental requirements

The first condition involves the technical requirements given in Table I-1. The second condition involves the potential market and cost of the battery. Economic incentives for industry by the government may be necessary in the preliminary stages of commercialization. The third condition involves the safety in vehicle crashes, the environmental impact, and the resource utilization of the battery. A paper is being written on these three conditions. The following schedule for the commercialization of the lithium/metal sulfide battery is developed in this paper:

1.	Complete van tests with the Mark I battery	July 1979
2.	Initiate design of a pilot-plant	Aug. 1979
3.	Initiate the development of an automated manufacturing plant	Aug. 1980
4.	Complete van tests with the Mark II battery	Aug. 1981
5.	Produce batteries for the BEST Facility	1982
6.	Initiate pilot-plant cell production	Oct. 1982
7.	Initiate in-depth market testing	Nov. 1982
8.	Complete car tests with Mark III battery	1983
9.	Initiate manufacture of cells in automated plant	Jan. 1987

B. Battery Safety
(A. A. Chilenskas)

A preliminary assessment† of the safety requirements for a lithium-aluminum/iron sulfide battery for an electric vehicle has been completed. The

*Consultant to ANL.

†Work carried out under the sponsorship of the ERDA Division of Transportation Energy Conservation by the Budd Company.

test results for a modified van, modified automobile, and advanced design automobile are discussed in a report issued by the Budd Company. Several of the important findings of this study are:

1. Three Li-Al/FeS_x cells at operating temperature were crushed, and the contents exposed to an air atmosphere. None of the cell materials showed any sign of reaction. These tests suggest that even under extreme accident conditions, such as the rupture of the cell containers, the active materials will not react with the air atmosphere. The implications of these tests for the safe deployment of lithium/iron sulfide batteries in electric vehicles are encouraging.

2. The cells are capable of absorbing their own kinetic energy from a crash into a barrier at 30 mph. The implications of this result are that battery configurations are possible that protect the vehicle occupants without placing severe restrictions on the design of the vehicle.

3. A conceptual design of an "optimum electric vehicle" was completed by Budd. A cylindrical battery 36 cm (14 in.) in diameter mounted in the central tunnel of a vehicle was selected for this design. An interesting variation on this design is the use of a rectangular "backbone" that is part of the vehicle frame and also serves as the outer vacuum jacket for the battery. These vehicle designs have provisions for decoupling the battery from the main frame at about 10 G, thus reducing the inertial force during crash conditions.

Domestic vans with a wheel base of approximately 275 cm (109 in.) and a GM Chevette were selected by Budd as suitable for conversion to propulsion by a 45-60 kW-hr battery.

III. INDUSTRIAL CONTRACTS

Nearly half of the ANL battery program consists of subcontracts with industrial firms. The purposes of the industrial subcontracts are to: (1) transfer the ANL technology to industry, (2) augment the base technology at ANL, (3) develop sources for materials and components, (4) develop procedures for production of cells and batteries, and (5) fabricate test cells and batteries. The major industrial subcontractors are Atomics International, Carborundum Co., Catalyst Research Corp., Eagle-Picher Industries, Inc., and Gould Inc.

A. Cell and Battery Development Contracts

1. Gould, Eagle-Picher, and Catalyst Research Contracts
(R. C. Elliott, R. F. Malecha, W. R. Frost)

Gould Inc., Eagle-Picher Industries, Inc., and Catalyst Research Corp. are involved primarily with the development and fabrication of cells that are tested either at ANL or in their own laboratories.

Fabrication of 55 upper-plateau* FeS_2 cells has almost been completed by Gould Inc. A problem with the feedthrough in the first one of these cells delivered to ANL was discovered by the Materials Group (Section VI.C.1). Correctional measures are being taken by Gould Inc. The following other activities were conducted at Gould this quarter: (1) completion of a facility for filling cells with electrolyte, (2) installation and check out of a 10-cell test facility, and (3) design of an uncharged FeS cell that should produce increased specific energy.

Production of cells is continuing at Eagle-Picher Industries, Inc. The FeS and FeS_2 cells originally required under their 58-cell contract have been delivered, and 14 cells have recently been added to the contract. The additional cells were requested by ANL after a prototype cell was found to have excellent performance. Further discussion of these cells appears in Section IV.A.1. Work also continues on the design of dies for the new 500-ton (4.5×10^5 kg) press needed to produce 13 × 18 cm cold-pressed electrodes. Installation of the press is in progress.

The second phase of the design and development of the hardware for the 30 kW-hr electric vehicle battery has nearly been completed.† An additional requirement was recently placed upon the design of the system. The battery, and especially the housing, is now to be designed for vehicle roadworthiness. The design of an acceptable bus bar and a method for fastening the bus bar to leads were also completed.

At Catalyst Research, testing of an upper-plateau FeS_2 cell with dip-cast negative electrodes and an Eagle-Picher positive electrode was terminated after two cycles, owing to an equipment malfunction that destroyed the cell. During break-in, the cell had a capacity of about 32 A-hr at a

---

*The voltage *vs.* capacity curves for FeS_2 cells show two voltage plateaus at about 1.65 and 1.35 V, respectively.

†A joint effort between ANL and Eagle-Picher.

3-hr rate (43% utilization). A post-test examination disclosed considerable swelling in the positive electrode. An additional upper-plateau FeS_2 cell is being constructed with carbon-bonded positive and dip-cast negative electrodes; this cell is being designed to achieve a high power density.

Ten lithium-aluminum electrodes fabricated by Catalyst Research using their dip-casting technique have been received. They will be assembled into various types of cells for further testing.

2. Mark IA Battery Contract

An advertisement soliciting expressions of interest in the development of a 40 kW-hr battery (Mark IA) will be placed in the *Commerce Business Daily*.

3. Atomics International's Contract

A Li-Si/FeS cell (1 kW-hr) equipped with 24 thermocouples located in selected positions within and outside of the cell was cycled through a programmed series of charge and discharge rates. External and internal temperatures, as well as the cell current and voltage, were monitored using a Hewlett-Packard data acquisition system, Model 3052A, which determined the cell capacity, coulombic efficiency, and energy efficiency for each cycle. The internal resistance was measured by periodic current interruption.

An analytical model of the thermal and electrical characteristics is being prepared using the data generated in these experiments. Temperature gradients within the cell were never more than a few degrees, even at the highest rate used (approximately the 5-hr rate). The cell temperature dropped during charge and rose during discharge in accordance with previous predictions based on entropy measurements. The reversible heat flow contribution from the entropy of the cell reactions is, therefore, large relative to those derived from irreversible resistance and electrochemical energy losses.

The model is being developed to predict cell performance characteristics including:

1. Active material utilization *vs.* load
2. Coulombic and energy efficiency *vs.* load
3. Performance under constant power conditions
4. Thermal control requirements

Fabrication of a Li-Si/FeS cell (2.5 kW-hr) was started during this period. The positive electrodes used a new vertical rib structure which offers advantages in cost and ease of assembly over earlier structures which used a honeycomb core. The test equipment and the test facility for this cell have been built and installed. The cell will be started up in early November 1977.

B. Battery Systems Contracts
(W. H. DeLuca, F. Hornstra)

Lead-acid batteries were obtained for a Renault electric vehicle, and the vehicle is now operational. Blake Electronics of Milwaukee was contracted to build a battery charger similar to that used in the Sears XDH-1 Electric Vehicle for use in the Renault. This charger is light in weight, inexpensive, and efficient.

A Fiat 850T electric van was obtained on a temporary basis to determine the feasibility of using it as a test bed for LiAl/FeS batteries.

IV. INDUSTRIAL CELL AND BATTERY TESTING
(W. E. Miller, E. C. Gay)

Testing of industrially fabricated lithium-aluminum/metal sulfide cells and batteries assembled from these cells is continuing. As improvements in cell designs are demonstrated, these are incorporated into the industrial cells. Fabrication of equipment for testing these cells and batteries continues. This equipment includes a facility to test a 60 kW-hr battery and another facility to test up to 100 cells.

A. Testing of Eagle-Picher Cells

(R. C. Elliott, P. F. Eshman, W. E. Miller, V. M. Kolba, G. W. Redding, W. W. Lark, R. Sink,* J. L. Hamilton)

A performance summary of Eagle-Picher cells operated during this quarter is presented in Appendix A. Some cells in the following discussion are referred to as baseline cells, *i.e.*, they have been qualified by testing a series of cells with the same design to obtain baseline performance data. These baseline cells contained FeS_2 thin (Type 2A) and thick (Type 2B) electrodes as well as FeS thin (Type 1A) and thick (Type 1B) electrodes. For further discussion of Eagle-Picher Industries' baseline cells, see ANL-76-98, pp. 15-17. Design modifications have been made on these baseline cells, and the effects of these modifications were determined by comparing cell performance with baseline data. In additional cell tests, the effects of environmental conditions and charging modes on cell performance were determined.

1. Qualification Tests

The modified FeS and FeS_2 cells were divided into nine groups (Items 1 to 9).† The Type I-1 and I-2 groups were built primarily to test Y_2O_3 felt separators in Type 1B baseline cells. Six of these cells were operated, and all of them developed short circuits in the separator in less than 2000 hr. The fragile Y_2O_3 felt separator was concluded not to be suitable for use in this cell design. The Type I-3 FeS cells were made with higher negative-to-positive capacity ratios (1.13 to 1.33) than that of the Type 1B baseline cells (1.0). Type I-3-A cells were the first contractor-produced cells to incorporate a 6.4-mm (1/4-in.) positive terminal rod in the feedthrough instead of the 4.8-mm (3/16-in.) lead used in baseline cells. This change had no significant effect on performance. Type I-3-B cells had a thinner positive electrode (5.6 mm) and denser, thinner negative electrodes (6.6 mm) than those of Type 1B baseline cells. No significant improvement in cell performance was achieved with this design. Type I-3-C cells were built with thinner (4.2 mm) and denser positive electrodes. The Type I-3-C cell had the highest specific energy of any contractor-produced FeS cell to date--50 W-hr/kg at the 4-hr rate.

Type I-4 cells were built to test the effect of moving the positive terminal rod from the center line of the FeS_2 cell to a position near one edge

---

*Cooperative Program Student.

†Discussion of the Item 1 to 4 cells is presented in greater detail in ANL-77-35, pp. 19-20 and ANL-77-68, pp. 16-18.

of the electrode.* The performance of these cells was poorer than that of the baseline cells. Postoperative examination of one of the Type I-4 cells, Cell EP-I-4-1, by the Materials Group indicated a more uneven utilization of the electrodes than that of baseline cells. Item 5 cells were Type 2B baseline cells obtained for battery tests (see Section IV.B).

Type I-6 cells were fabricated to evaluate a number of design changes from Type 2B baseline cells, and were expected to deliver high specific energies. This cell design used a thinner, denser positive electrode (4.0 mm), an oversize negative electrode utilizing waste space near the edge of the can, 55 at. % Li-Al, and no ZrO_2 retainer cloth. The expected specific energy of these cells was 85 W-hr/kg at the 4-hr rate; however, this value was achieved only at the 10-hr rate. Although the thickness of the positive electrode in the Type I-6 cells was approximately the same as that in the Type 2A baseline cells, the capacity loading of the baseline cells was only one-half that of the Type I-6 cells. The lower capacity loadings in the baseline cells permitted them to have higher volume percentages of electrolyte (78% for Type 2A baseline cell *vs.* 65% for Type 6 cell). This reduction in electrolyte volume in the Type I-6 cells greatly reduced the utilization of the positive electrode material. For example, in the Type 2A baseline cells the utilization was 74% at a current density of 56 mA/cm^2, whereas the utilization dropped to 57% for the same current density in Type I-6 cells. More information is needed on the relationship between electrolyte volume and percent utilization to obtain specific energy optimization in this cell design.

Type I-7 cells are a considerable departure from the Type 2B baseline design. This design includes a one-piece positive electrode (5 mm thick) and a flexible connection between the positive terminal rod and the current collector. The flexible connection minimizes stresses on the molybdenum weld. This design lowered the cell resistance to 7-8 mΩ (baseline cell, 8-9 mΩ). Type I-7 cells have achieved the highest specific energy of any contractor-produced cell to date, 80 W-hr/kg at the 4.5-hr rate. With minor mechanical changes to reduce the cell weight by about 10%, the specific energy is expected to increase to 90 W-hr/kg at the 4-hr rate and the peak specific power to 75 W/kg. The cell performance curves for the Type I-7 cells are given in Figs. IV-1 and IV-2.

Eagle-Picher Industries, Inc. is now building Type I-8 cells. Owing to the high performance of the Type I-7 cells, the design for 14 of the 34 Type I-8 cells will be variations of the Type I-7 design. All fourteen of these cells will use a screen across the positive side of the separator. In some of these cells, the honeycomb current collector in the negative electrode will be eliminated.

2. Cell Testing in Air Environment

The long-term effect of air on an operating cell is being determined to assess cell performance in the event of leakage in a secondary container. Cycling of EP-2B8, which is an FeS_2 cell wrapped in Kaowool and operated in

---

*In battery design work, the off-center position was discovered to be more desirable than the central location.

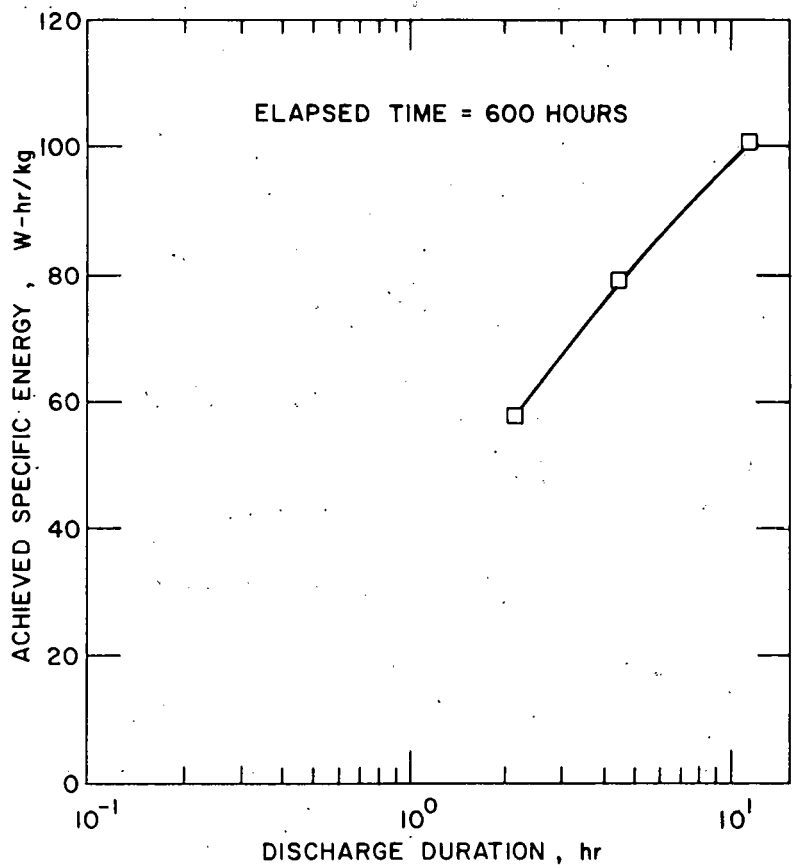

Fig. IV-1. Specific Energy of Type I-7 Cells During Discharge

air, was voluntarily terminated after 378 days of operation (533 cycles) owing to declining coulombic performance. The overall performance of this cell was not significantly different from that of Cell EP-2B6, which was operated in a helium atmosphere. This test demonstrates that operation of a cell in air over a long period of time does not have a deleterious effect on cell performance. Toward the end of the cycle life of EP-2B8, its capacity early in cell life (0.97 A-hr) could be nearly reproduced by using a 4-A charge and a 13-A discharge (initial discharge and charge rate, 13 A).

3. Charging Mode Studies

The FeS cell, EP-I-3-C-2, is being used to compare a current-limited, constant-voltage (CLCV) charge with a constant-current (CC) charge. This cell has a negative-to-positive capacity ratio of 1.33, a positive electrode thickness of 4.2 mm, and a negative electrode thickness of 7.0 mm. The constant voltage charge may be set to current limits up to 25 A, after which the current is reduced as required to maintain the constant voltage. The constant voltage is terminated when a minimum current (*e.g.*, 2 A) is reached.

Date for various charging tests on EP-I-3-C-2 are presented in Table IV-1. The data show a saving in charge time of approximately 49% using the 20 → 2 A CLCV charge rather than the 10-A CC charge, with only a 4%

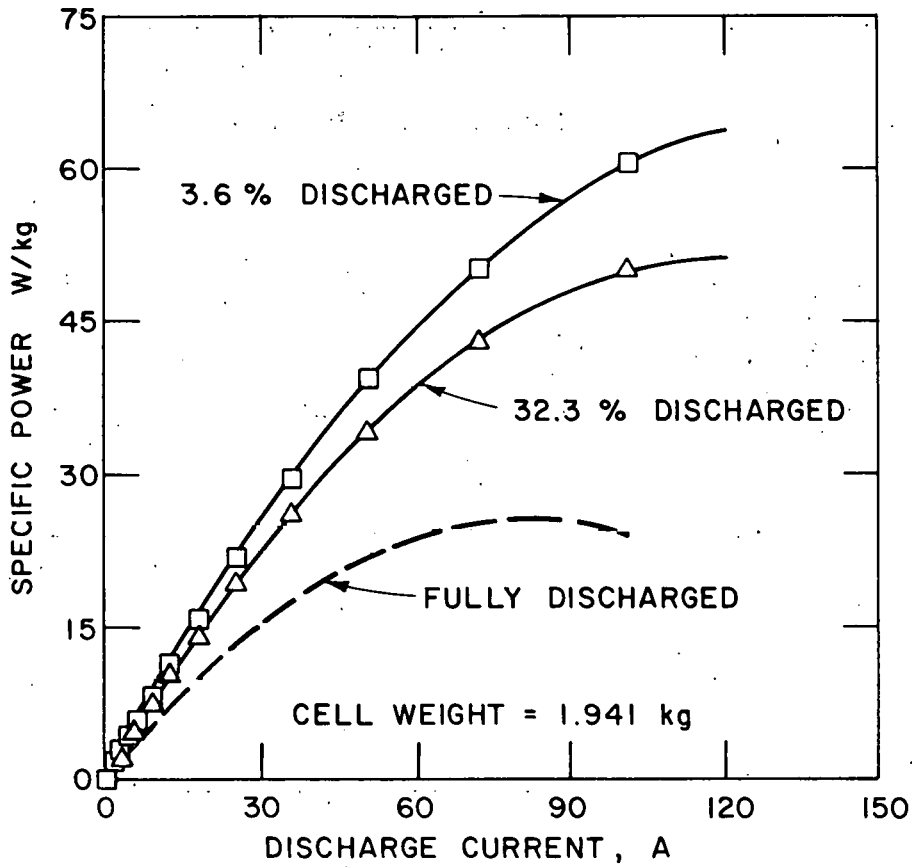

Fig. IV-2. Specific Power of Type I-7 Cells During Discharge

reduction in performance. This cell's performance has been declining with increased cycling, and some of the subtle effects of charge modes are difficult to interpret. For example, recent measurements of a 25-A CC charge show a 13% decline in energy from that of the earlier measurements on the 25-A CC. Plans are to repeat the charging-mode tests to determine how cell performance is affected by time of operation.

Table IV-1. Charging Test Data for Cell EP-I-3-C-2

Charge Mode[a]	Current, A	Capacity, A-hr	Energy, W-hr	Charge Time, hr
CC	10	68.3	84.6	6.7
CLCV	10 → 2	66.4	82.1	7.1
CC	15	65.6	79.8	4.4
CLCV	15 → 2	67.7	83.9	5.4
CLCV	20 → 2	65.9	81.5	3.4
CC	25	59.9	79.9	2.3
CLCV	25 → 2	63.6	78.6	4.0

[a]Discharge current, 10 A. A minimum of 4 and a maximum of 12 cycles were used for each charge measurement.

B. Battery Testing

(V. M. Kolba, G. W. Redding, J. L. Hamilton)

The battery testing efforts are directed toward the development and evaluation of battery configurations and designs. Start-up and conditioning methods are also being investigated. Cells are being tested in both series and parallel arrangements. The following battery tests are listed in chronological order.

1. Two-Cell Battery Test

Testing of FeS Cells EP-1B4 and 1B6 in series (designated Battery B7-S) has continued at the 10- and 5-hr rates, with and without equalization. Although equalization is very beneficial to cells having high coulombic efficiency, these tests indicate that equalization charging has only marginal benefits for cells that have high self-discharge rates. The total battery resistance remains about the same (26 mΩ) as early in life. Without equalization, the capacity has declined from its peak value by ∿42% at the 10-hr rate and ∿40% at the 5-hr rate. With bulk charging only, the coulombic efficiency is about 87% and the energy efficiency is about 70%. The coulombic and energy efficiencies decrease when the equalization charge is utilized. Bulk charge refers to the first part of the charge period, in which most of the total ampere-hours are charged at high currents. This is followed by the equalization period, in which a small amount of charge is added at a low current.

The specific energy is ∿34 W-hr/kg at the 10-hr rate and ∿26 W-hr/kg at the 5-hr rate. This battery has now operated for more than 477 days and 756 cycles. Cell 1B4 has operated for more than 526 days and 789 cycles.

2. Five-Cell Battery Test

As discussed in ANL-77-68, p. 23, problems were experienced with testing of the five-cell battery (designated B12-S). The performance declined to the point where the battery voltage near the end of discharge was less than 1.75 V. The battery was shut down after 34 cycles and the cells examined. No obvious cell failures or faults were found and the range of cell resistances (through the mica sheets used for insulation) was high, *i.e.*, no cell had been short-circuited. Little oxidation was observed on the copper bus bars at the bar-to-cell interfaces; this indicates that the battery case was airtight. The five cells were individually cycled at the 7.5-A rate. During cycling, Cell EP-I-5-3 did not maintain voltage during charging and EP-I-5-8 did not charge above 1.8 V. The other three cells were charged, and then operated for a minimum of two cycles to determine their performance. Performance data are given for these five cells in Table IV-2.

3. Three-Cell Battery Test

Three cells from Battery B12-S (EP-I-5-4, -5, -7) were connected in series and placed in an insulated case to form a battery (designated B13-S). This battery is being cycled at about 420°C. Testing has been conducted at discharge currents of 7.5, 10, 15, 20, and 25 A using charge currents of 7.5 and 10 A. Performance data for Battery B13-S are presented in Table IV-3. A comparison was made between the individual performance data in Table IV-2 and performance data for the same three cells in Battery B13-S. This

Table IV-2. Performance Data for Cells of Battery B12-S

Cell No.[a]	Capacity, A-hr	Energy, W-hr	Efficiency, % A-hr	Efficiency, % W-hr	Resistance,[b] Ω
I-5-3[c]	-	-	-	-	15
I-5-4	83.9	125	99	85	3800
I-5-5	93.9	137.3	96	79	550
I-5-7	83.9	121.8	98	80	8.5
I-5-8[d]	-	-	-	-	21

[a]All cells fabricated by Eagle-Picher Industries, Inc.

[b]At room temperature.

[c]Did not maintain voltage during charge.

[d]Did not charge above 1.8 V.

Table IV-3. Performance Data for Battery B13-S

Current,[a] A		Specific Energy,[b]	Energy
Discharge	Charge	W-hr/kg	Efficiency, %
7.5	7.5	51	82
10	10	41	78
15	10	32	71
20	10	27	68
25	10	23	64

[a]A minimum of 5 cycles at each current.

[b]Includes cell weight only: battery case, supporting structure, and wiring not included.

comparison indicated that at a current of 7.5 A the capacity declined by 11% and the energy by 14% when these cells were in B13-S.

The cell resistances for Battery B13-S are high, 11-12.6 mΩ, whereas the interconnection and lead resistances are only about 0.4 mΩ. The high cell resistances are reflected in the poor battery performance at high currents.

The discharge cutoff voltage was decreased from 1.0 to 0.9 V and the charge cutoff voltage was increased from 2.0 to 2.1 V. This change resulted in a slight (5%) gain in specific energy. The specific energy is 47 W-hr/kg at the 10-hr rate. The energy efficiency is 79% and the coulombic efficiency is >99%.

C. Equipment for Cell and Battery Tests

1. Testing Facilities for Cells and Batteries

(G. W. Redding, J. L. Hamilton, R. Alford,* V. M. Kolba, W. E. Miller)

Preliminary start-up tests of a multicell-test heating chamber (manufactured by Huppert) have been made. This chamber has provisions for the simultaneous testing of eight cells. The system is now operational except for its automatic atmosphere-control system. Cell EP-I-3-B-2, which was previously used for qualification testing, is being used to aid in check-out of the multicell test chamber. This cell has been connected to a minicycler and the appropriate data aquisition system input and operated for 3-5 cycles to assure that the cyclers, leads, and acquisition system are functional. All remaining minicycler data acquisition interfaces will be checked sequentially using this cell.

Static testing of large-scale (30-60 kW-hr) batteries is being planned. Equipment, instrumentation, and support equipment have been specified and are in the process of being procured. Present plans call for the installation and check-out of this equipment by the middle of 1978. During this period the power supplies and data-acquisition and computer-control systems were specified and are being ordered. Drawings were completed for the Mark 0 - Mark I equalizer system (for laboratory tests) and power supplies have been procured for this system.

Plans are also being made to build a 100-cell test facility. This facility will be used to determine product and performance reliability prior to the procurement of large numbers of cells for the electric-vehicle battery. Testing will be oriented toward lifetime testing of large numbers of identical cells supplied by several vendors. Design and fabrication of an economical 75-A cycler for the facility have been initiated. Scoping of the data-acquisition system and interfacing with a central computer system are being reviewed.

2. Battery and Cell Cyclers

(E. C. Berrill, W. W. Lark, C. A. Swoboda, F. Hornstra)

A programmable 100-A cell/battery prototype cycler was designed and constructed by the Electronics Division of ANL. The cycler is undergoing check-out tests. Another eight units are presently under construction, and are about 40% completed.

Design and construction drawings of the 25-A minicyclers were updated to include all prevailing refinements so that additional units could be constructed by an outside vendor.

Bids for battery cyclers were reviewed for the testing of the Mark I battery. Various computer configurations and systems were reviewed and recommendations made.

---

* Industrial participant from Eagle-Picher Industries, Inc.

3. Charging Systems for Electric Vehicle Batteries
(W. H. DeLuca, F. Hornstra)

A computer analysis of two battery chargers was conducted to study ambient temperature and high temperature batteries. Neither charger contained a transformer. The source of power was ac line voltage without an interceding transformer. One charger supplied with the Renault electric vehicle uses a fixed resistor for current limiting and a mechanical relay for charge cut-off voltage. The other charger uses a silicon controlled rectifier (SCR) whose conduction time is varied during the half-wave cycle. This system is used on the Sears electric vehicle. The analysis showed that the SCR unit exhibits higher energy efficiency but has larger ac currents. Both units would provide higher efficiency with the addition of an inductive filter. The efficiency of the resistor-controlled unit will go from its present 50% to about 65% at 3.5-A currents with the addition of a filter, whereas that of the SCR-controlled unit will go from 75-90% to 89-97% with a filter at 5-A currents. The SCR unit also provides more versatility because the conduction can be controlled electronically. The study is continuing to determine the increase in efficiency as a function of the size, weight, and cost of a filter, and to analyze other types of battery chargers. Data obtained from subsequent operation of the charger on the Renault electric vehicle showed almost exact agreement with the above analysis.

V. CELL DEVELOPMENT AND ENGINEERING
(E. C. Gay, H. Shimotake)

The effort in this part of the program is directed toward improving the performance and lifetime of lithium-aluminum/metal sulfide cells at ANL. Technical advances resulting from this effort will be incorporated into the cells that are fabricated by industrial firms. Work during this period was concentrated on the development of metal-sulfide cells that are adaptable to the electric-vehicle application, with emphasis on high specific energy at high rates. A summary of performance results of the test cells is presented in Appendix A.

A. Positive Electrode Development

1. Cells with Hot-Pressed Electrodes
(L. G. Bartholme, F. J. Martino, E. C. Gay, and H. Shimotake)

An uncharged, upper-plateau FeS_2 cell, R-30, was operated and tested. To prevent the formation of Li_2S in the separator (ANL-77-35, p. 48), a Hastelloy B screen was added to the positive electrode; this lowered the sulfur-to-metal ratio from 2.0 to 1.75. The percent utilization of this cell was excellent, 88% at the 5-hr rate and 76% at the 2-hr rate. However, this cell developed a short circuit after 48 days (70 cycles) of operation. The cause of cell failure will be determined by the Materials Group.

Cell chemistry studies (Section VII.B.2) indicate that NiS_2 may be an attractive alternative to FeS_2 as the active material in the positive electrode. Cyclic voltammetry has shown apparent kinetic hindrance in the charge reaction of the FeS_2 electrode that is not evident in the case of NiS_2. Consequently, two uncharged Li-Al/NiS_2 cells, R-31 and -32, have been operated and tested. Carbon powder (Union Carbide, C-34) that had been heated previously to 1000°C was added to the positive electrode mixture of Cell R-32 to help current collection. Both cells have shown excellent coulombic efficiency (>99%), thereby indicating reversibility of the cell reactions; however, superior performance was achieved by Cell R-32. The performance of these cells at various discharge rates is given in Fig. V-1. Cell internal resistance for R-32 was much lower than that of R-31, 4.5 *vs.* 12 mΩ. This difference is attributed to the addition of the carbon powder that had been treated at high temperatures (see Section V.A.2).

Post-test examinations of FeS_2 cells by the Materials Group showed that gradual losses in capacity are partially due to sulfur transport from the positive electrode and subsequent formation of Li_2S in BN fabric or Y_2O_3 felt separators. In addition, semiconductive Y_2O_2S has been found to form in Y_2O_3 felt separators. To prevent this migration problem, Cell M-4 (uncharged) was built with a positive electrode containing a reduced sulfur-to-metal capacity ratio (1.5 instead of 2.0). This electrode was hot-pressed from a mixture of 40 vol % FeS_2-NiS-Fe-Mo* and 60 vol % LiCl-KCl, and enclosed by a molybdenum frame and screen assembly. A BN felt separator/retainer was initially used in the cell because it is more amenable to bending than Y_2O_3 felt or BN fabric. Start-up of Cell M-4 proved to be difficult, and the

*See section V.A.3 for explanation of why molybdenum was used.

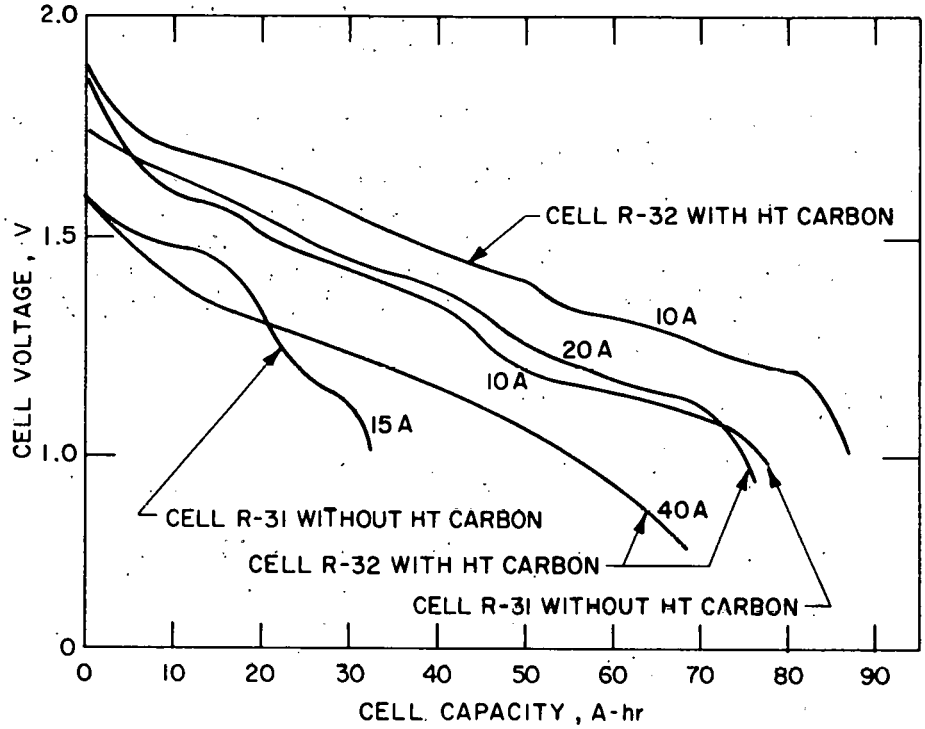

Fig. V-1. Performance of Cells R-31 and R-32 (HT = heat treated)

start-up problem was attributed by the Materials Group to the poor wettability of BN felt by the molten salt.

Cell resistances of 25 mΩ were typical during the first 20 cycles of operation; but after repeated degassing at 460°C the resistance decreased to 3.5 mΩ. The peak capacity of Cell M-4* was 144 A-hr with an 8-A (30 mA/cm^2) current and 135 A-hr with a 15-A (56 mA/cm^2) current. The specific energy was 116 W-hr/kg with an 8-A current and 109 W-hr/kg with a 15-A current. After 27 cycles the cell developed a short circuit, and operation was temporarily terminated. The cell was then reconstructed with a Y_2O_3 felt separator and restarted. Performance was completely recovered by this rebuilt cell.

2. Cells with Carbon-Bonded Electrodes
(T. D. Kaun, W. Borger†)

Cell KK-11, a carbon-bonded FeS_2 cell with a Y_2O_3 felt separator, was discussed in ANL-77-68, p. 29. This cell had a design similar to that of Cell M-3 (ANL-77-68, p. 28), except that M-3 has a hot-pressed positive electrode. Operation of KK-11 was voluntarily terminated after 223 cycles and 120 days. Throughout its lifetime, Cell KK-11 maintained stable capacity at high discharge rates (up to 150 mA/cm^2). At termination, capacity loss was

*Theoretical capacity: positive electrode, 267 A-hr; negative electrode, 165 A-hr.

†Industrial Participant from Varta Batteries, A. G., Germany.

less than 11% of its 70 A-hr peak capacity (theoretical capacity, 75 A-hr) with a 14-A (50 mA/cm^2) current. Coulombic efficiency and energy efficiency were 90 and 76%, respectively. Post-test analysis by the Materials Group showed the same amount of Li_2S in the separators of KK-11 and M-3. Because of the difference in cell lifetimes (M-3, 55 days; KK-11, 120 days), it was suggested that the Li_2S forms in the separator of this type of cell up to a certain level and thereafter the reaction ceases. Other than increasing the cell resistance from 3.6 to 4.5 mΩ in KK-11, the Li_2S did not appear to produce any highly adverse effects on cell performance. Formation of Y_2O_2S was also observed in the separators of these two cells. This suggests that Y_2O_3 felt separators may be unsuitable for FeS_2 cells.

Another carbon-bonded FeS_2 cell with a Y_2O_3 felt separator, KK-12, was built and placed in operation. This cell had a TiS_2 facial layer on the positive electrode to prevent the transport of sulfur from this electrode, but developed a short circuit after 35 cycles. After the cell was dismantled, bright yellow areas were observed in the Y_2O_3 felt separator, indicating the presence of escaped sulfur. Recent work by the Cell Chemistry Group has identified greater sulfur losses from TiS_2-FeS_2 mixtures than from other sulfide mixtures.

Experiments on small-scale cells (electrode area, 20 cm^2) are being undertaken to further define the optimum parameters for the preparation of carbon-bonded electrodes. Cells with 16 vol % carbon in their positive electrodes had resistances of 40-45 mΩ, whereas those with 8 vol % carbon had resistances of 50-60 mΩ. Start-up problems were encountered when graphite powder and carbon powder (Ketzen black EC) were used in these cells. These problems were attributed to gas absorption. Of the cells tested, those using carbon fibers (Union Carbide) produced the best utilization with low resistance.

In the preparation of carbon-bonded electrodes, large amounts of carbon are added to the active material. The larger part of this carbon is bound by furfural alcohol resin at temperatures below 500°C. However, the electronic conductivity of carbon formed from organic material at this temperature is known to be low as compared with that of the iron sulfides used in the positive electrodes of Li-Al/FeS_x cells. High conductivity carbon can be formed only by heating the carbon material to 1000°C or higher. In an experiment, carbon powder (Union Carbide C-34) was heated for 2 hr to 1050°C under helium; this thermal treatment decreased the resistance of this material by a factor of 400. This high-temperature-treated carbon was then tested in the positive electrodes of small-scale FeS cells. In one cell, KB-7, the positive electrode was fabricated by pressing a mixture of active material, high-temperature carbon (7.8 vol %) and electrolyte; no organic binder was used. The performance of this cell was equivalent to that of another cell with a carbon-bonded electrode containing 6.1 vol % high-temperature and 0.6 vol % low-temperature carbon, active material, electrolyte, and organic binder (furfural resin). This suggests that high-performance positive electrodes can be economically fabricated from a pressed mixture of active material, high-temperature carbon, and electrolyte.

3. Cells with Pellet Electrodes
(R. Thompson,* P. F. Eshman†)

Pellet electrodes are fabricated by cold-pressing small plaques or pellets from a mixture of active material and electrolyte, and these pellets are then slipped into a welded grid structure of metal channels. In ANL-77-68, p. 25, the pellet design was investigated as an alternative method of fabricating FeS electrodes with large areas. The good performance of cells of this type encouraged the investigation of FeS_2 pellet-electrode cells.

Cell PFC-3-01,‡ built with a positive electrode of FeS_2-CoS_2 pellets, has now operated for 29 cycles (23 days). The cell required five cycles for break in, probably due to its thick pellets (no center current-collector sheet was used in the positive electrode). During operation, the utilization dropped from 89.5 to 58.6%, coulombic efficiency from 98.1 to 94.8%, energy efficiency from 70.9 to 62.7%, and specific energy from 72.0 to 60.5 W-hr/kg. Internal resistance was high throughout operation (13.0 to 25.8 mΩ), and this high resistance was attributed to a poor weld connection between the molybdenum grid structure and the terminal rod.

Because of the high cell resistance of PFC-3-01, the grid structure prepared for PFC-4-01 has been modified. The new pellet-grid design is illustrated in Fig. V-2. These design changes are expected to alleviate the stress on the grid-to-terminal rod connection and to provide better conductivity for the cell. This design requires approximately 60% less molybdenum than used for the current collector in the Type 2B baseline cell.

Tests were conducted on small-scale test cells with molybdenum additives. These tests indicated that the addition of molybdenum powder (-200 mesh) to an FeS_2-CoS_2 electrode results in improved performance and reduced electrode expansion. With 9.3 vol % molybdenum added to an FeS_2-CoS_2 electrode, capacity increased by 6%, energy increased by 4%, and expansion decreased by 68%. The addition of molybdenum in the form of MoS_2 to FeS_2-CoS_2 electrodes was also found to reduce expansion. Construction of pellet-electrode cells with molybdenum additive are planned.

B. Testing of Cells with Negative Electrode Additives
(F. J. Martino, H. Shimotake)

Engineering-size FeS-Cu_2S cells are being operated to evaluate the effects of the addition of a third metal to Li-Al alloy electrodes. These cells have negative electrodes in which pyrometallurgically prepared Li-Al and an additive are loaded into iron Retimet current collectors.

Tests of a baseline cell with no additive, FM-0, have been terminated after 263 cycles (136 days). During the first 200 cycles, cell capacity declined by only 6% from its peak capacity of 52 A-hr (61% negative electrode

*Industrial Participant from Gould Inc.

†Industrial Cell and Battery Group.

‡Theoretical capacity: negative electrode, 150 A-hr; positive electrode, 159 A-hr.

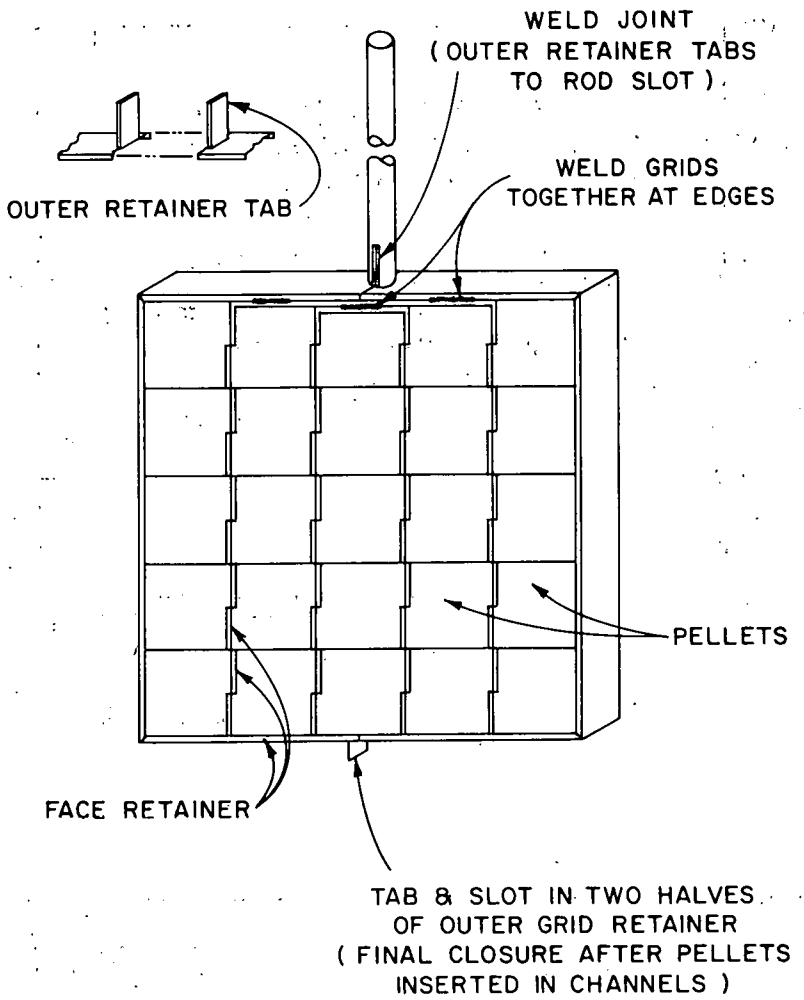

Fig. V-2. Design of Positive Electrode for Cell PFC-4-01

utilization). The cell has been submitted to the Materials Group for post-test examination. Cells FM-1 (Li-Al-In), FM-2 (Li-Al-Cu), and FM-3 (Li-Al-Sn) were reported in ANL-77-68, p. 31. Cell FM-4, which has 5 wt % zinc added to the Li-Al electrode, has operated for 70 cycles and 40 days. In this time, its peak capacity of 51 A-hr (63% negative electrode utilization) has declined by ∿3.5%. This cell and the baseline cell (FM-0) show very similar performance characteristics, thereby indicating little benefit from the use of zinc additive. A performance summary of the FM-series is given in Fig. V-3 and Table V-1.

Owing to the good performance of Cell FM-3, an FeS_2 cell utilizing Li-Al alloy with a tin additive (8.6 wt %) was placed in operation. At the 5-hr rate with a current of 12.5 A (43 mA/cm^2), Cell FM2-1 demonstrated an average voltage of 1.52 V and a specific energy of ∿48 W-hr/kg. At the 2.5-hr rate with a current of 23 A (80 mA/cm^2) and a 1.0 V (IR included) cutoff voltage, the cell capacity was 61 A-hr, the average discharge voltage was 1.48 V, and the specific energy was 48 W-hr/kg. After 182 cycles and 104 days, the capacity at the 5-hr rate declined from its peak of 61 A-hr by almost 30%, and the

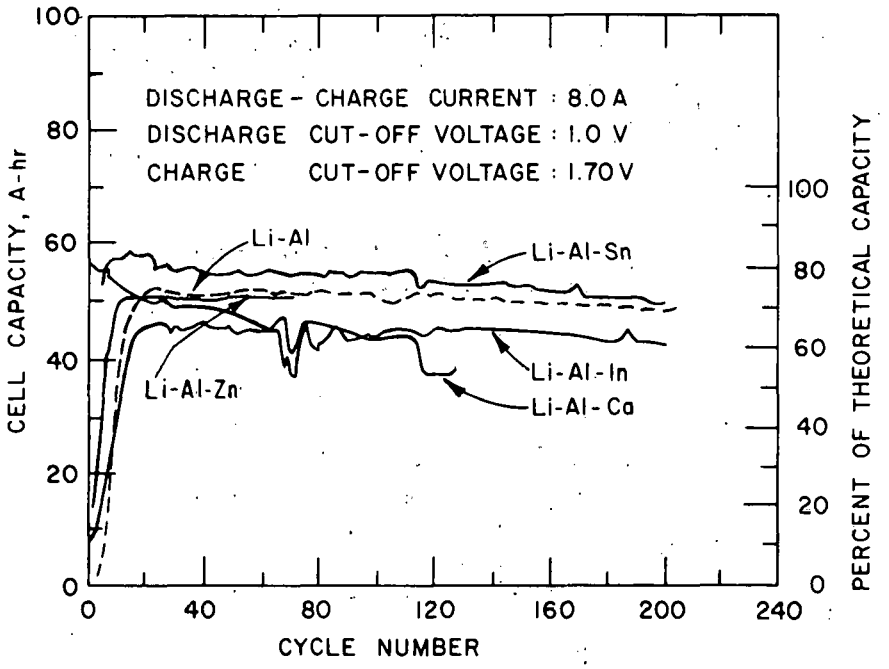

Fig. V-3. Cell Capacity *vs.* Cycle Number for FM Cells

Table V-1. Performance of FM-Series Cells

Cell	Description	Neg. Electrode Capacity, A-hr		Neg. Utilization,	Max. Energy,	Capacity Decline, %		Operating Time		Resistance,
		Theor.	Max.	%	W-hr	100 cycles	Final	Cycles	Days	mΩ
FM-0,	Li-Al/FeS-Cu_2S	85	52	61	65	1	5.8	200	136	6.5-6.8
FM-1,	Li-Al-5 wt % In/ FeS-Cu_2S	85	46	57	57	4	8.5	200	98	6.8-7.0
FM-2,	Li-Al-8 wt % Ca/ FeS-Cu_2S	90	56	71	69	21	34	127	77	6.5-6.8
FM-3,	Li-Al-8.6 wt % Sn/ FeS-Cu_2S	86	57	73	71	3.5	14	200	117	6.8-7.0
FM-4,[a]	Li-Al-5 wt % Zn/ FeS-Cu_2S	85	51	63	63	3.5	-	70	40	6.8-7.1

[a]Cell still in operation.

resistance increased from 6.5 to 7.8 mΩ. At this point, cell performance appears to have stabilized, although a coulombic efficiency of 93% indicates a possible short circuit. The anticipated stabilizing effects of the tin additive on cell capacity are not apparent in this cell. Testing of Cell FM2-1 will continue. A baseline, upper-plateau FeS_2 cell will be run for comparison purposes in the near future.

C. Testing of Cells with Alternative Separators
(T. W. Olszanski and H. Shimotake)

Three engineering-scale cells containing ceramic-powder separators are being evaluated. These are engineering-scale FeS_2 cells in which all-powder separators are used to replace the BN fabric separator and zirconia cloth particle retainer. All cells were made by a two-step operation in which the separator and negative electrodes were hot-pressed onto a prepressed positive electrode and the resulting plaque was placed in a can and sealed. The major advantages of the powder separator are low cost and ease of fabrication. Two cells, PW-1 and PW-2, had Y_2O_3 powder separators and the third cell, PW-3, had a MgO powder separator. Cells PW-1, -2, and -3 had relatively short lifetimes: 57 days and 116 cycles, 36 days and 50 cycles, and 34 days and 69 cycles, respectively. However, these three cells produced high coulombic efficiencies and low internal resistances (average 10 mΩ) prior to the end of cell lifetime.

An engineering-size cell (PW-6) was built with a MgO powder separator that was filled by a vibratory technique. Temporary spacers located between the positive and negative electrode faces were used for loading the powder. Cell PW-6 lasted only three cycles. The failure was due to mechanical failures of the powder separator. The necessary corrections in the design will be made in the next cell.

VI. MATERIALS DEVELOPMENT

Efforts in the materials program are directed toward the development of various cell components (electrical feedthroughs, electrode separators, current collectors, and cell hardware), testing and evaluation of cell materials (corrosion and wettability testing), and post-test examinations of cells to evaluate the behavior of the electrode and construction materials.

A. Development and Fabrication of Cell Components

1. Electrical Feedthrough
(K. M. Myles and J. L. Settle)

The corrosive environment within Li-Al/LiCl-KCl/FeS_x cells precludes the use of any commercially available electrical feedthrough. Accordingly, a program is under way to develop a feedthrough that is compatible with the cell materials, leak tight, inexpensive, and compact. The best long-term solution may be a brazed-seal feedthrough, but to date no reliable ceramic-to-metal braze has been found (ANL-77-17, p. 39).

Coors Porcelain has produced preliminary test samples of yttria coated with several nonmetallic brazes. These samples have satisfactorily withstood the cell environment. Unfortunately, as reported in ANL-77-68, p. 36, short-circuiting developed across the ceramic in the early stages of in-cell corrosion tests. The cause of the short circuit has been traced to small additions that were made to the yttria body to increase the strength of the brazed joint. Coors is uncertain as to whether satisfactory composites can be made if the additive is removed. Accordingly, work on development of a nonmetallic braze has been suspended until this matter can be resolved.

ILC Technology intends to examine the effects of sophisticated feedthrough designs in an attempt to minimize corrosion. This program, which is concerned with FeS_2 cells, will closely interact with one sponsored by Atomics International and the Electric Power Research Institute at ILC to develop a feedthrough for FeS cells.

A major advancement was made in the design of the ANL mechanical-seal feedthrough. The new design was conceived after observing that compressed BN powder springs back (about 20% longitudinally) after the compacting load is removed. A drawing of this new feedthrough design is shown in Fig. VI-1. In this new design, a snap retainer ring is pressed into the feedthrough housing as the BN sealant powder is being compressed. When the powder is fully compressed, the retainer ring engages a groove in the feedthrough housing, thereby preventing the BN powder from expanding longitudinally. One of the advantages of the retainer-ring feedthrough is ease of assembly. In addition, the height and weight of the feedthrough are reduced from those of previous designs utilizing threaded nuts (Conax) or crimp seals. The length of the new feedthrough is 2.5 cm, the diameter is 1.9 cm, and the total weight is only 32 g (conventional Conax feedthrough, 126 g). Experiments to determine the assembly specifications are under way. Preliminary measurements yielded a leak rate of 9.5×10^{-5} Pa·m^3/s. In similar fashion to the crimp seal feedthrough, this new design allows for the addition of a secondary solder glass seal, which would greatly decrease the above leak rate. The cost for manufacturing the

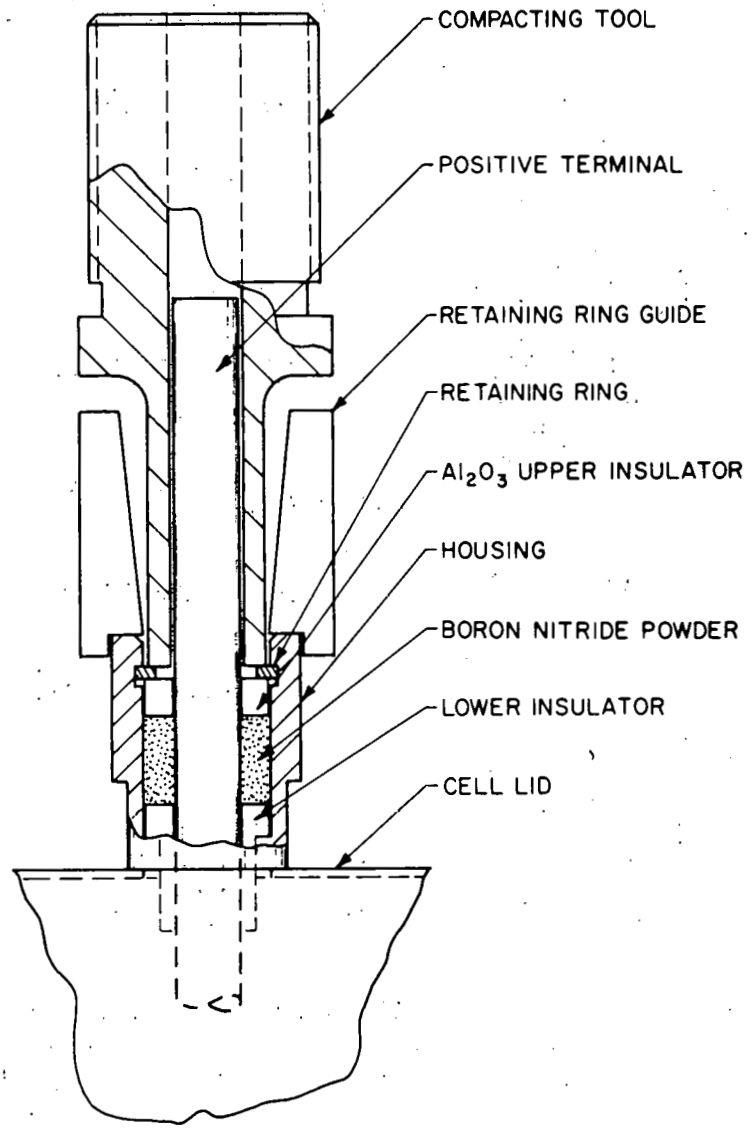

Fig. VI-1. Mechanical Feedthrough with a Retainer Ring

feedthrough is about $2.00 each in units of 1000. In-cell testing of a retainer ring feedthrough is planned.

2. Electrode Separators
(R. B. Swaroop and C. W. Boquist)

Felt, powder, and paper separators are being developed as alternatives to the BN fabric currently used in lithium-aluminum/metal sulfide cells. The development of BN felt has been emphasized because it is technically superior to other available forms of separators, and has low cost potential. Powder separators are also being investigated because they have the lowest cost potential. During this quarter, two separator materials, BN felt and MgO powder, were evaluated in small-scale (7.6 × 12.7 cm) prismatic Li-Al/FeS test cells. A schematic drawing of the test cell is shown in Fig. VI-2. This cell configuration was selected because it closely approximates that of

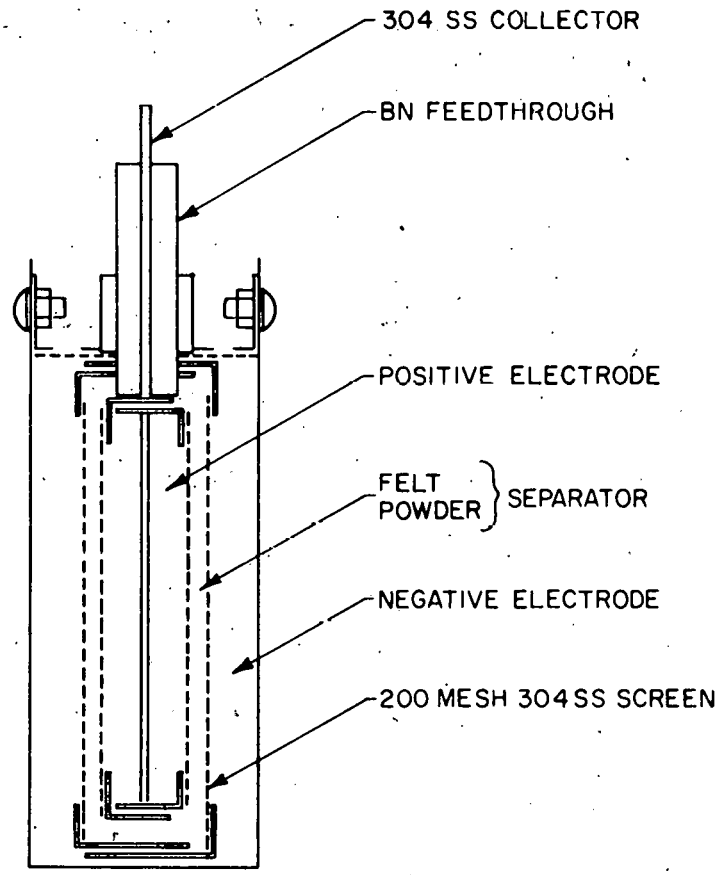

Fig. VI-2. Cell for Testing Separators

engineering-scale cells, and meets the mechanical requirements for the successful application of felt and powder separators. This test was designed to make a comparison of cells using felt and powder separators under similar conditions.

The BN felt was obtained from the Carborundum Company* and was stabilized at high temperatures in a nitrogen atmosphere before use. Because this felt was very weak,† two 1-mm-thick layers were used for the separator. The cell (SC-19) was assembled in the 50% charged condition, and has been in operation for 120 days and 195 cycles. The performance of the cell, *i.e.*, the active material utilization and coulombic efficiency, is shown in Fig. VI-3. The performance of this cell has been more stable than that of any previous separator test cell. During the first 60 cycles, both the charge, and discharge current densities were increased in steps of 20 mA/cm^2, from 40 to 120 mA/cm^2. For cycles 60 through 100, the charge current density was held at 40 mA/cm^2 and the discharge current density was again increased in steps of 20 mA/cm^2 from 40 to 120 mA/cm^2. As shown in Fig. VI-3, the percent

*The development of BN felt separators was initiated by a contract funded by ANL.

†Stronger felts are now available.

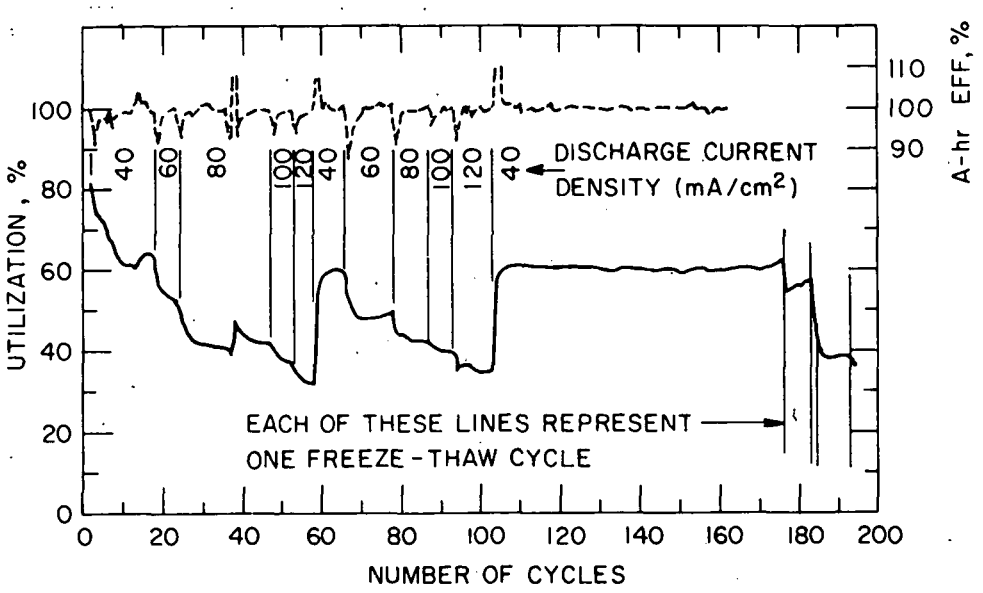

Fig. VI-3. Electrical Performance of Cell SC-19 with BN Felt Separator

utilization decreased from 60 to 35% under both sets of cycling conditions. These results show that the cell utilization was unaffected by the charge rates used in these tests. From cycle 100 to 175 the charge and discharge current densities were maintained at 40 mA/cm^2. During this period, the utilization and the coulombic efficiency remained constant at about 60 and 100%, respectively. Between cycles 176 and 195, the cell was allowed to cool to ambient temperature and was then reheated to 450°C four times. The cell capacity decreased after each thermal cycle as shown in Fig. VI-3. By the end of the third thermal cycle the percent utilization had decreased to about 38% at the charge-discharge current density of 40 mA/cm^2. Thus, the freeze-thaw cycles appear to have a deleterious effect on cell performance.

Magnesium oxide powder was tested as a separator in Cell SC-21. The cell design was essentially the same as that of SC-19 except that the picture frame and screen assembly were replaced with frames and screens enclosing each negative electrode. This arrangement allowed the electrodes to be positioned properly in the cell prior to vibratory loadings of MgO powder. The MgO powder (-60, +120 mesh, >99% purity) was obtained from the Cerac Company. The cell was assembled in a 50% charged state with a 1.8-mm-thick powder separator. So far, the cell has been in operation for 29 days and 67 cycles. At a discharge current density of 40 mA/cm^2, the utilization of this cell was about 60%. However, as the discharge current density was increased, the utilization dropped sharply (about 15% at 100 mA/cm^2).

The utilizations as a function of discharge current density for Cells SC-19 and SC-21 are shown in Fig. VI-4. This figure shows that the utilizations of these two cells are approximately the same at low discharge current densities (about 80% at 20 mA/cm^2 and 60% at 40 mA/cm^2); however, at higher discharge current densities, the performance of the MgO-powder cell decreased much more sharply than that of the BN-felt cell.

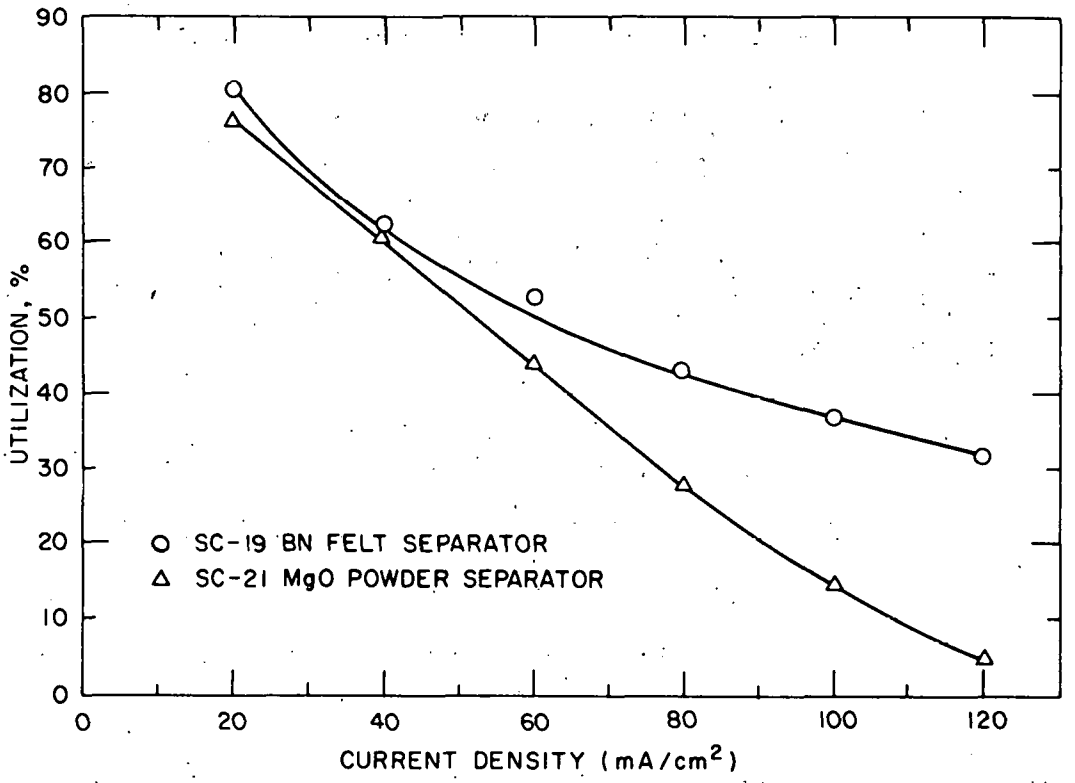

Fig. VI-4. Performance of Cells SC-19 and SC-21 as a Function of Discharge Current Density

In addition to in-cell evaluations of recommended materials, out-of-cell tests are used to screen candidate materials. Preliminary experiments were conducted to determine the compatibility of CaF_2 with LiCl-KCl eutectic, LiAl alloy plus LiCl-KCl eutectic, and lithium metal at 450°C for 300 hr. X-ray diffraction analysis* performed on the solidified reaction products indicated the following results: (1) precipitation of LiF in the salt; (2) the formation of $CaAl_2$ and LiF, thus indicating that LiAl alloy reacted with CaF_2; and (3) the formation of LiF on the surface of the CaF_2 crystals immersed in lithium. From these tests, it was concluded that CaF_2 is not compatible with the cell environment and is not a suitable separator material.

Post-test examinations of cells have indicated that a major mode of cell failure is short-circuiting caused by the extrusion of active material through retainer weaknesses at the edges or corners of electrodes (see Section VI.C.1). The apparatus shown in Fig. VI-5 was used to observe the flowability (creep) behavior in powder separators and electrode-separator systems in the absence of discharge-charge cycles. The specimen studied was a 10.6-mm-thick, compacted MgO powder pellet saturated with 29 vol % LiCl-KCl eutectic salt. The test was conducted in a helium atmosphere under a static load of 700 kPa (100 psi). Figure VI-6 shows the thermal expansion data obtained from this test. The thermal expansion of the MgO pellet is almost linear up to 350°C; the measured thermal expansion coefficient is 9×10^{-6}/°C in this temperature

*B. S. Tani, Analytical Chemistry Laboratory, ANL.

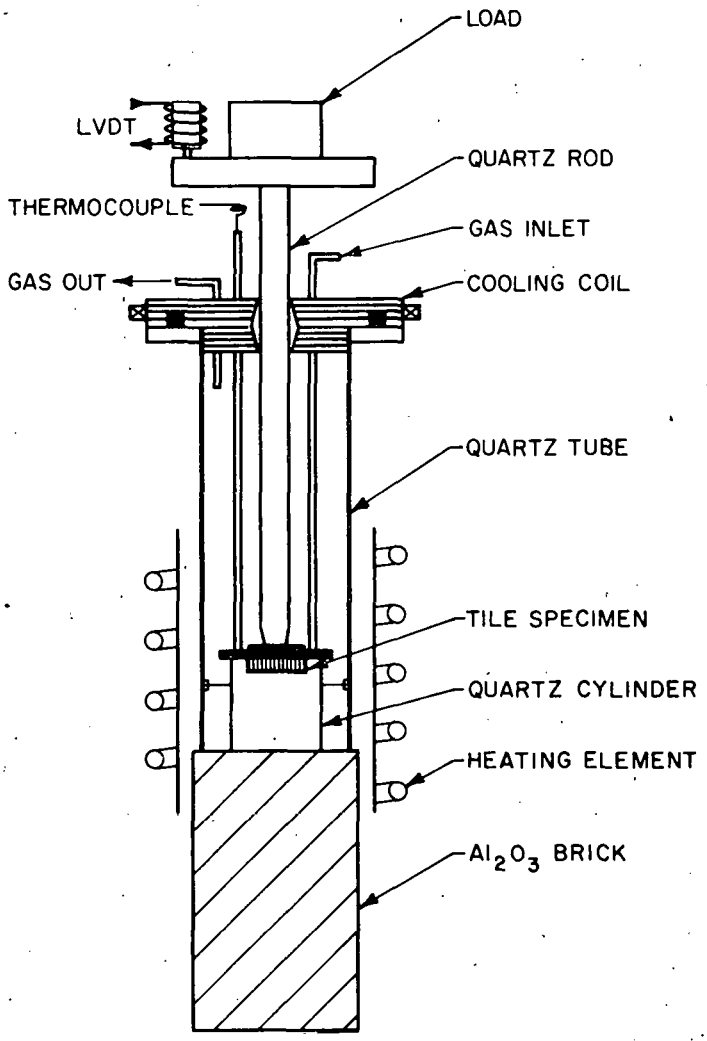

Fig. VI-5. Modified Static Creep Apparatus (LVDT = Linear Voltage Differential Transducer)

range. The thermal expansion coefficient of pure MgO is $13.0 \times 10^{-6}/°C$.[1] At the melting point of the eutectic salt (350°C) a break is observed in the curve, and beyond that break thermal expansion of the MgO pellet increases linearly up to 450°C. At this temperature, the measurements were conducted isothermally for 275 hr. The MgO pellet crept about 10 μm (0.09%) in the first 140 hr of this test; however, it stabilized after that interval. The flow rate (creep rate) calculated from these data was 7×10^{-6} m/m per hour. This test clearly indicates that under compressive stresses as small as 500-1000 kPa, an initial movement will occur in the powder particles of a MgO separator. This movement will lead to further densification of the separator layer in the cell. Further tests of MgO powder are planned.

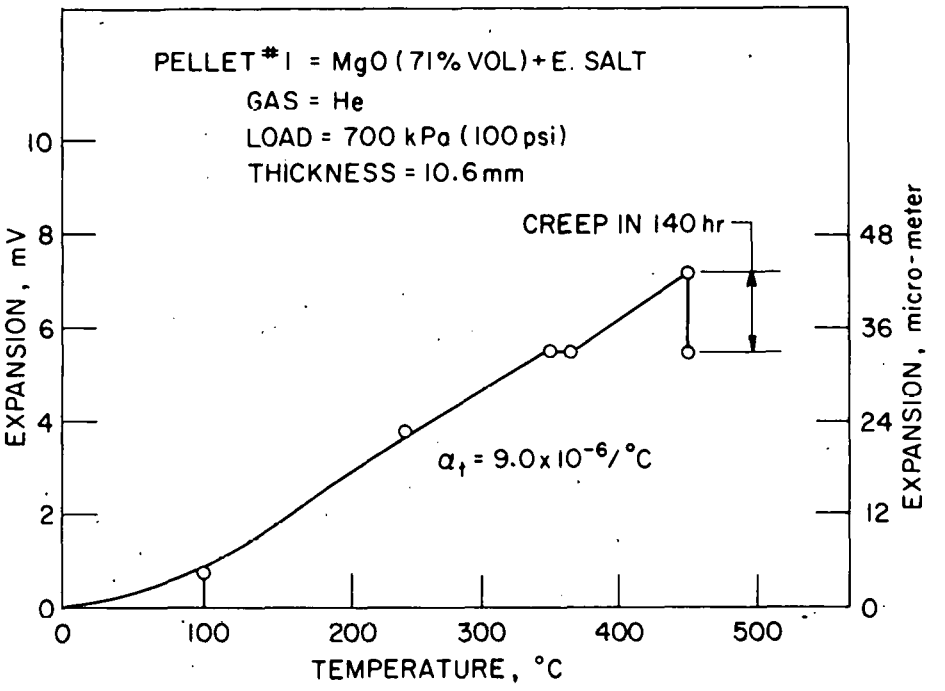

Fig. VI-6. Expansion Curve of Dense MgO Pellet (10.6 mm thick) Saturated with LiCl-KCl Eutectic

3. Ceramic Materials
(T. D. Claar and J. T. Dusek*)

Rigid, porous ceramic bodies are under consideration as alternative separators, and several approaches to fabricating this type of material are under investigation. Yttria is the ceramic material currently being studied. Porous Y_2O_3 specimens with total porosities ranging from 55 to 85% were obtained by sintering bodies that were prepared by four different techniques: (1) pressing agglomerated Y_2O_3 particles to which organic binders had been added, (2) casting plasters that were made by mixing Y_2O_3 powder into a nitric acid solution, (3) blending pregenerated foam into a Y_2O_3 slurry containing dilute acid or some other setting agent, and (4) mixing a foaming agent in concentrated form directly into a slurry (*in-situ* foaming) and then casting.

Yttria separators were fabricated into rectangular shapes for testing in prismatic cells by two techniques. In the first technique, 12 wt % of an organic binder, consisting of acrylic resin and stearic acid in a 3:1 ratio, was added to as-received Y_2O_3 powder† in a slurry containing an excess of CCl_4 solvent, and the resulting yttria cake was crushed and sieved to several size fractions. Rectangular plates were pressed from three different size fractions in a 8.92 × 6.92 cm die at a pressure of 16.6 MPa (2400 psi) and sintered for 14 hr at 1500°C. Each of the four specimens appeared to be in very good condition after sintering, with no cracking or warping. Dimensional, linear shrinkage, and density data for the sintered plates are given in Table VI-1. Geometric densities range from 39 to 44% of theoretical density(TD), and linear shrinkages range from 5.5 to 6.9%. Slightly larger shrinkages and higher densities were associated with the finer agglomerates. Flat separator

*Materials Science Division of ANL.

†Molycorp, 99.9% Y_2O_3.

Table VI-1. Pressed-and-Sintered Y_2O_3 Separator Plates

Plate No.	Agglomerate Size Fraction, Mesh	Dimensions, cm			Average Linear Shrinkage, %	Geometric Density, % TD[a]
		Length	Width	Thickness		
PS-1	-20+60	8.4	6.55	2.6	5.5	39
PS-2	-60+100	8.35	6.5	1.5	6.3	41
PS-3	-100	8.3	6.45	2.3	6.9	43
PS-4	-100	8.3	6.45	2.2	6.9	44

[a]Percent of theoretical density.

plates that are 1 to 2 mm thick will be prepared by the pressing-and-sintering technique for in-cell testing.

Separators have also been prepared by casting Y_2O_3 plaster formulations (method 2 above) into molds made of plaster of Paris and rubber. The 5-mm-thick shapes were rectangular (8 × 11 cm) with raised edges (6 mm high) that allow the positive electrode to be completely enclosed inside two separator halves. Six such separators were cast, dried overnight at room temperature, and then carefully heated to 170°C in a vacuum drying oven to remove additional water. The separators were then stacked two high and sintered at 1500°C for 12 hr. After sintering, one of the bottom plates was cracked, whereas the other two were in fairly good condition. The flat face of each of the upper plates was warped significantly due to downward sagging of this unsupported section during sintering. Linear shrinkages of 8 to 11% were measured for these pieces. The geometric density of a plaster test piece fired with these plates was 25% TD, indicating a substantially greater porosity than observed for the pressed-and-sintered separators. Currently, the procedures for casting, drying, and firing of foams and plasters with rectangular shapes--with and without raised edges--are being refined to provide the best possible separators for in-cell testing.

Effort is presently being directed toward characterization of porous separators. Characterization will include measurements of pore size and size distribution, density, and crushing and bending strength.

B. Testing and Evaluation of Cell Materials

1. Corrosion Studies

(V. A. Maclaren* and J. A. Smaga)

Previous studies (ANL-76-9, p. 44-46) have shown that the dissimilar metal reaction between the discharged Li-Al electrode (Li depleted) and cell components (iron- or nickel-base alloys) at the negative electrode potential results in the formation of Al-rich intermetallic layers. These brittle intermetallic layers undermine the structural integrity of the reacted cell

*Graduate student participant, North Dakota State University.

components, and this could result in failure of the cell. The source of the LiCl-KCl eutectic employed in these studies was found to have a significant influence on the rate of this dissimilar metal reaction. The reaction rate using LiCl-KCl eutectic from Anderson Physics Laboratories (APL) was often more than an order of magnitude higher than the rates found in similar tests using eutectic salt from the Lithium Corporation of America (Lithcoa). When dissolved in deionized water, the APL salt has a pH of 5.8 whereas Lithcoa salt has a pH of about 10. This series of tests was conducted to substantiate the influence that salt pH has on the dissimilar metal reaction rate.

In this period, metal couples of unalloyed aluminum and AISI 1008 low-carbon steel were subjected to static immersion tests at 450°C for 85 to 90 hr in various eutectic salts. Weight measurements on the individual aluminum and 1008 steel members were made both before and after exposure to the test environment. As shown by the test results in Table VI-2, the reaction rate was greatest for the couple tested in as-received APL eutectic salt. The following observations on the rate of aluminum pickup by the low-carbon steel were derived from this table: (1) the reaction rate is a factor of three lower in the as-received Lithcoa salt than in the as-received APL salt; (2) in filtered* Lithcoa salt, the reaction rate is one-third that in the as-received Lithcoa salt; and (3) the addition of 0.1 mol % KOH to APL causes a reduction in the reaction rate by a factor of 21 and the addition of 0.1 mol % KOH to filtered Lithcoa salt causes a reduction in the reaction rate by a factor of 6.5. The above observations, in particular the third one, confirm the suspicion (ANL-77-9, p. 45) that an anionic impurity (*i.e.*, the hydroxyl ion, OH^-) in the eutectic salt retards the kinetics of the dissimilar metal reaction through passivation of the aluminum surface.

Table VI-2. Dissimilar Metal Couple Tests at 450°C in as-Received and Modified Eutectic Salts

LiCl-KCl Eutectic	Weight Charge, mg/cm^2		Al Pickup Rate by Low-Carbon Steel, mg/cm^2·yr
	Al	1008 Steel	
APL (as-rec'd)	-1.84	+1.11	114
Lithcoa (as-rec'd)	-1.03	+0.36	37
Lithcoa (filtered)	-0.73	+0.13	13
APL + 0.1 mol % KOH	-0.30	+0.06	5.5
Lithcoa (filtered) + 0.1 mol % KOH	-0.36	+0.02	2.0
APL + Li-Al	+0.50	-0.02	0.0

*The purpose of filtering the Lithcoa salt is the removal of particulate impurities. However, this process causes a compositional shift because the Lithcoa salt is rich in LiCl. The filtered material is closer to the eutectic composition.

In the last entry of the table, a substantial amount of Li-Al powder was added to APL salt; this test confirmed the requirement of lithium depletion in the Li-Al alloy of the negative electrode. This addition successfully eliminated the reaction with iron. The iron member showed a small weight loss, whereas the aluminum showed a significant weight gain. With a source of lithium present, the aluminum reaction with the iron alloy is replaced by a second reaction between the aluminum and the Li-Al powder. Because it is likely that hydroxide ion would eventually enter into other side reactions within an actual cell, the last test suggests that excess lithium capacity in the negative electrode is a more certain way of suppressing the aluminum reaction with the iron alloy. Future work in this area will involve other alloy additions to the aluminum in an effort to achieve similar results.

2. Cell Wetting Studies
(J. G. Eberhart)

The internal resistance of a lithium/iron sulfide cell is determined in part by the extent to which the LiCl-KCl electrolyte fills the pores of the separator. Pore filling is, in turn, a function of the wettability of the separator surface. Wettability tests with molten LiCl-KCl eutectic have been completed on a series of rigid, porous Y_2O_3 separators (fabricated by W. Tuohig*). The specimens were sintered Y_2O_3 foams and powders. All of the specimens were easily penetrated by the molten salt. (Easy penetration implies that the advancing and receding contact angles are both less than 90°.) This conclusion is in accord with contact angle measurements previously made on near-theoretical-density Y_2O_3 plaques. A difference was observed in the time required for the penetration of the rigid Y_2O_3 foams and the sintered Y_2O_3 powders. The former required several hours for electrolyte infiltration of the structure; the latter required about one day. This difference in penetration time does not appear to be crucial for separator applications.

A new, 3-mm-thick, BN felt material has been obtained from Carborundum Corp. for use as a cell separator. This felt was used in the construction of Cell M-4 (see Appendix A for description of this cell), which exhibited a high initial internal resistance. This high resistance was attributed to poor electrolyte penetration of the BN felt. Because this felt appears to be an attractive electrode separator, its wetting characteristics were studied. Wettability testing showed that this BN felt, in similar fashion to BN fabric (ANL-77-35, p. 43), is penetrated with difficulty by molten LiCl-KCl. (Difficult-to-penetrate materials have an advancing contact angle larger than 90° and a receding contact angle smaller than 90°.) Even though this material is not easily penetrated by molten salt, once the electrolyte is forced into the pore structure it remains in place without continuous pressure. Since the BN felt is not less wettable than BN fabric, the source of the problem in Cell M-4 is probably the small amount of electrolyte used in the cell. The volume of electrolyte is a key wetting factor because the outer surfaces of the separator must contact at least a thin layer of electrolyte for evacuation and repressurization of the cell to cause penetration of the separator.

---

*Formerly in the Materials Science Division of ANL.

One method of wetting separators in cells having a small volume of electrolyte is the infiltration of the separator with electrolyte before cell assembly. Figure VI-7 shows a possible method of carrying out this procedure for a flat fabric or felt separator. The separator is held firmly between two steel frames. In the test chamber, the three-layer assembly is immersed into molten electrolyte, and the system is evacuated and repressurized with helium. The repressurization causes the infiltration of the separator by the electrolyte, except where the frame covers it. The assembly is then withdrawn from the salt bath and allowed to cool. The cooling process causes the infiltrated part of the separator to become rigid owing to the solidification of the salt in its pores. A separator can then be cut out from the infiltrated portion of the structure.

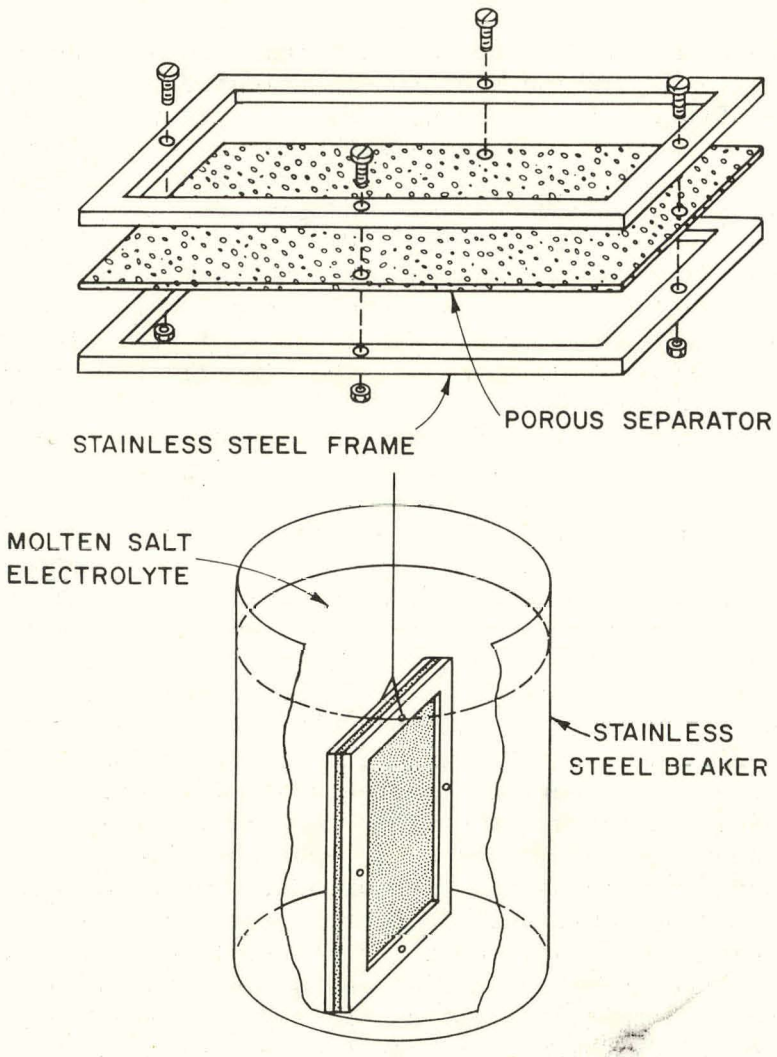

Fig. VI-7. Equipment for Infiltration of Separator with Electrolyte before Cell Assembly

A second method of improving separator wettability is the use of pretreatments on the BN felt. Various pretreatments were tested to see whether or not they could make the felt easy to penetrate by a molten salt. When a BN felt was immersed in molten $LiAlCl_4$ at 200°C, easy-to-penetrate behavior was observed. After this same felt was drained of the $LiAlCl_4$, it was easily penetrated by molten LiCl-KCl. In other experiments the following pretreatment salts were dissolved in a solvent at room temperature: (1) $LiAlCl_4$ in benzene, (2) $LiAlCl_4$ in toluene, (3) LiCl in methanol, (4) KCl in methanol, and (5) $LiAlCl_4$ in methanol. After BN felt separators were soaked in these various solutions, the solvents were removed (by evacuation) from the separators. None of these (room temperature) pretreatments improved the wettability of the BN felt. This study is being continued with other solvents.

3. Cell Degassing
(J. G. Eberhart)

The degassing and attendant pressure build-up which can occur during the operation of a cell is probably detrimental to its efficiency and lifetime. Thus, a study was initiated to characterize, by mass spectrometry, the gaseous species produced while cells are in charge, discharge, or open-circuit mode.

Since the last report, the quadrupole mass spectrometer has been tested. In addition, several fittings have been fabricated for the introduction of gas samples into the spectrometer.

The sampling of the gaseous species produced by engineering-scale cells will be carried out in a helium-atmosphere glovebox. These analyses will be the "blanks" against which samples from cells will be compared. Sampling flasks have been fabricated.

C. Post-Test Cell Examinations
(F. C. Mrazek, N. C. Otto, J. E. Battles)

Post-test examinations are conducted on test cells primarily to evaluate the performance of various construction materials--in particular feedthroughs, current collectors, electrode separators, and cell housings. These examinations provide important information, not only on the compatibility of cell components with the cell environment, but also on the performance and behavior of the lithium-aluminum and metal sulfide electrode materials. The examination procedures were described in a previous semiannual report (ANL-8109, p. 72).

1. Summary of Post-Test Cell Examinations

Table VI-3 presents the results of the cell examinations that were performed during this period, along with some conclusions as to the causes of cell failure. The cells that were examined included vertical, prismatic engineering cells and small test cells (KB and TK series). Two ANL cells are of particular interest. Cell CB-1 was operated longer than any previous vertical, prismatic cell (552 days). The positive electrode was carbon-bonded chalcopyrite ($CuFeS_2$) rather than the usual FeS. The cell was operated as an open cell in a metal beaker, and examination revealed unusually large amounts of metallic copper in the separators. Cell YF-1 utilized 55 at. % Li-Al negative electrodes and an FeS_2 positive electrode vibrationally loaded into Hastelloy B foam metal. Metallographic examination showed only a minor

Table VI-3. Summary of Post-Test Examinations

Cell Number	Type of Cell	Cell Lifetime		Reason for Termination	Post-Test Observations
		Days	Cycles		
YF-1	Li-Al/FeS_2-CoS_2	294	610	Fracture of positive electrode current conductor rod	Purpose: to test 55 at. % Li-Al, constant voltage charging, Hastelloy B foam current collector in carbon-bonded positive electrode, and Y_2O_3 felt as separator. Positive lead fractured because of intergranular corrosion. Hastelloy B foam in positive electrode completely reacted. The resulting decline in sulfur activity probably accounts for small amount (compared with typical FeS_2 cell) of Li_2S in separator. Y_2O_3 separator reacted to Y_2O_2S. A 325-mesh screen without any ZrO_2 cloth retainer effectively contained negative active material, which had a very fine and uniform porous microstructure (iron retimet current collector.
CB-1	LiAl/$CuFeS_2$	552	1006	Test completed. Declining coulombic efficiency.	Carbon-bonded chalcopyrite ($CuFeS_2$) used as positive material. Corrosion rate of low-carbon steel current collector, 84 μm/yr. Unusually large amounts of metallic copper found in separator (this probably caused minor multiple conductive paths between electrodes). Thickness of electrodes doubled.
G-04-008A	LiAl/FeS_2-CoS_2	31	30	Short circuit	Li_2S in separator. Negative electrodes compressed in thickness from 0.9 cm to 0.6-0.7 cm. Most of the area of the two Mo current collector tabs (near weld area that joins current collector sheet to current collector rod) fractured. Short circuit in feedthrough caused by migration of zinc from solder glass. Also, insulators badly cracked owing to excessive pressure used in fabrication of feedthrough.
EP-I-4-1	Li-Al/FeS_2-CoS_2	39	42	Short circuit	Purpose: to test offset positive terminal. Short circuit caused by positive honeycomb current collector cutting through separator and contacting negative retaining screen. Offset positive terminal appeared to decrease positive electrode utilization. A higher-than-usual level of SiO_2 contamination in positive. In addition to typical Li_2S in separator, minor amounts of unidentified phase in separator.
2B-Fe-1	LiAl/FeS_2-CoS_2	27	29	Short circuit	Both these cells had sacrificial metal screen added to front of positive electrode to change sulfur/metal ratio from 2.0 to 1.75. Reduced sulfur activity expected to reduce amount of Li_2S that forms separator. Examination showed that both screens totally reacted and that Li_2S in separator considerably reduced.
2B-Ni-1	LiAl/FeS_2-CoS_2	34	48	Short circuit	Short circuits caused by positive honeycomb current collector cutting through separator and contacting negative electrode.
KK-11	LiAl/FeS_2-CoS_2	119	223	Test completed	Purpose: to evaluate Y_2O_3 felt separator and carbon-bonded positive electrode. Some of Y_2O_3 felt separator reacted with sulfur to form Y_2O_2S. Only two of six current collector tabs still joined to current collector rod.
FM-0	LiAl/FeS-CuS_2	136	263	Test completed	Mild steel honeycomb in positive electrode reduced by corrosion to one-half its original thickness (corrosion rate, 89 μm/yr).
PW-1	Li-Al/FeS_2-CoS_2	57	116	Short circuit	Purpose: to test Y_2O_3 powder separator and "electrolyte starved" cell. Short caused by non-uniform expansion of electrodes which extruded positive active material through separator and into contact with negative electrode. Y_2O_3 powder separator reacted to form Y_2O_2S. A heavy Li_2S layer in separator. The negative electrode had "V"-shaped notches which appeared to cause breaks in separator.

Table VI-3. (contd)

Cell Number	Type of Cell	Cell Lifetime Days	Cell Lifetime Cycles	Reason for Termination	Post-Test Observations
PW-2	Li-Al/FeS_2-CoS_2, uncharged	36	50	Short circuit	Purpose: to test Y_2O_3 powder separator. Several short circuits through separator. Y_2O_3 powder separator reacted to form Y_2O_2S. This reaction had sintering effect which made separator rigid. Uneven expansion of both electrodes broke up rigid separator, thereby allowing penetration of positive active material into negative electrode. Heavy Li_2S layer in separator with less associated free iron than normal.
PW-3	Li-Al/FeS_2-CoS_2, uncharged	34	69	Short circuit	Purpose: to test MgO powder separator. Near short circuit caused by non-uniform expansion of both electrodes leading to thinning of powder separator. Its MgO powder separator was reacted in low resistance areas; very heavy Li_2S layer observed.
TO-6	Li-Al/FeS_2-CoS_2, uncharged	29	35	Short circuit	Purpose: to test BN felt separator, Li foil-Al wire as negative electrode, and Hastelloy B frame in positive. Short circuit caused by corrosion of spot welds of the Mo retaining screen to Hastelloy B frame. Failure of screen allowed extrusion of positive active material which contacted negative electrode. Two bands of Li_2S and large crystals of Al_2S_3 found in BN felt separator only, near shorted area. The BN felt performed well as did Li foil-Al wire negative electrode.
M-3	LiAl/FeS_2-CoS_2	58	92	Poor efficiency	Multiple sectioning revealed electrical resistance between electrodes of <100 Ω. X-ray diffraction of Y_2O_3 felt separator showed significant amount of Y_2O_2S.
KB-2	LiAl/FeS-Cu_2S	27	50	Short circuit	Small-scale cell. Steel housing of positive electrode shifted and contacted negative electrode, thereby causing short circuit.
KB-3	LiAl/FeS-Cu_2S, (pyrolitic carbon)	50	147	End of test	Small-scale cell. Carbon distribution in this cell very good. In contrast to cell KB-2, no carbon agglomerates observed.
TK-18	Li-Al/FeS	21	50	End of test	Small-scale, carbon-bonded cells. Built to test the effect of changes in particle size and carbon content in positive electrodes. All four positive electrodes had high utilization. Decreasing particle size of starting active mix improved utilization, particularly at high current densities. An apparent decline in utilization noted with high carbon content. Microscopic examination revealed very uniform current collection.
TK-19	Li-Al/FeS	22	37	End of test	
TK-20	Li-Al/FeS	27	53	End of test	
TK-21	Li-Al/FeS	23	53	End of test	

amount of Li_2S in the separator, much less than observed in typical FeS_2 cells with molybdenum current collectors. Cell failure was caused by intergranular corrosion of the nickel rod used for the positive electrode terminal.

A Gould FeS_2 cell (G-04-008A) failed because of a short circuit in the Gould-type feedthrough. Post-test examination of the feedthrough showed that its complete length had been penetrated by electrolyte. In addition, excessive cracking of the lower Y_2O_3 and upper Al_2O_3 insulators and shearing in the BN powder seal were observed; the cracking and shearing indicate that the pressures used during fabrication (~520 MPa) were excessive. Further examination of the BN powder seal revealed a dark material at the Al_2O_3 insulator/BN powder seal interface. X-ray diffraction of this material indicated the presence of metallic zinc in addition to the expected BN. X-ray fluoresence* confirmed the presence of zinc. The source of zinc was traced to the solder glass (Corning type 7574) used to make the external seal on this feedthrough. The zinc was either vapor-deposited at the Al_2O_3 insulator/BN powder seal interface during thermal treatment to seal the solder glass or it was leached from the solder glass by electrolyte.

2. Separators of FeS_2 Cells

Post-test examinations have shown a large amount of Li_2S in the electrode separator of all FeS_2 cells except Cells S-86, S-87 (see ANL-77-35, p. 48), and YF-1. These three cells utilized nickel and/or Hastelloy B, rather than molybdenum, for current collectors in the positive electrode. This behavior suggested that the formation of Li_2S in the separator is related to the high sulfur activity in FeS_2 cells. To check this, Cell 2B-Ni-1 was fabricated with a sacrificial screen of nickel and Cell 2B-Fe-1 with a screen of iron in order to decrease the sulfur-to-metal ratio from 2.0 (normal FeS_2 cell) to 1.75.† The results of sulfur analyses‡ of the separators from these two cells and from four typical FeS_2 cells are listed in Table VI-4 and show a much reduced sulfur content for Cells 2B-Fe-1 and 2B-Ni-1. The amount of Li_2S observed microscopically in the separators of Cells 2B-Ni-1 and 2B-Fe-1 was also much less than that observed in typical FeS_2 cells.

Because the Li_2S appears to form a nearly continuous band in the separator, the thickness of this band could be measured. From these measurements, a calculation** was made of the total volume of Li_2S and the amount of sulfur in the separator. The average thickness of the Li_2S layer was 0.2 mm and the average area was 312 cm^2. Assuming that the Li_2S is 90% dense (a reasonable estimate according to metallographic examinations), the calculations yield 6.5 g of sulfur in the separator. This value is in reasonable agreement with the value of 6.0 g of sulfur in the separator of Cell EP-2A4 which was determined by several chemical analyses. This level of sulfur accounts for 14.5-15.6 wt % of the total sulfur loaded into the positive electrodes.

---

*Analyses performed by M. Homa of the Analytical Chemistry Laboratory.

†Cells prepared by the Industrial Cell Development Group at ANL.

‡Analyses performed by K. Jensen and R. Crooks of the Analytical Chemistry Laboratory.

**Based on measurements of five different cells.

Table VI-4. Sulfur Content of Electrode Separators in FeS_2 Cells

Cell Number	Sulfur, wt %
2B-Fe-1	1.01
2B-Ni-1	3.59
EP-2A4	6.38
EP-2B6	6.68
EP-I-4-1	10.11
M-3	8.31

In addition to the formation of Li_2S in the separators of FeS_2 cells, examinations have identified Y_2O_2S as a reaction product in cells that employed Y_2O_3 separators (powder or felt). Thus far, this reaction product has been isolated in six cells--five FeS_2 cells (Cells YF-1, M-3, KK-11, PW-1, and PW-2) and one FeS cell (SC-18). The effects, if any, that the formation of Y_2O_2S has on cell performance has not been determined.

3. In-Cell Corrosion Results

In-cell corrosion data on current-collector materials have been obtained from the metallographic examinations of both positive and negative electrodes. These results are important for predicting the expected lifetime of construction materials. In the cells examined, the current-collector material for the negative electrode was low-carbon steel, which is attacked by aluminum (Li-depleted LiAl). In the positive electrode, low-carbon steel was used as the current collector material in FeS cells and molybdenum as the current collector material in FeS_2 cells. Previous static corrosion tests (ANL-77-17, p. 39) indicated that these materials are attacked by the sulfur-active materials and that FeS_2 is the more corrosive of the two iron sulfides.

The corrosion rate for the aluminum reaction with the low-carbon steel current collector ranges from 25 to 85 μm/yr penetration, and appears to decrease with longer operating times. For the FeS positive electrode, the corrosion rate for the low-carbon steel ranges from 50 to 125 μm/yr penetration, and appears to be independent of time. These corrosion rates were obtained from the examination of seven cells with operating times of 15 to 552 days. Molybdenum current collectors in the positive electrodes of five FeS_2 cells show evidence of only minor sulfide attack, with the corrosion rate ranging from 2 to 4 μm/yr penetration.

4. Causes of Cell Failure

An important function of post-test cell examinations is the determination of cell failure causes and the subsequent recommendations for corrective action. The causes of failure have been reviewed for vertical, prismatic cells. The initial results were previously reported in ANL-77-68, p. 43, for a total of 48 cells. An additional 13 cells have been examined in this period.

The combined results are summarized in Table VI-5. The corrective actions previously recommended (ANL-77-68, p. 46) for the major causes of cell failure remain valid.

Table VI-5. Cell Failure Mechanisms

Cause of Failure	Cases
Extrusion of electrode material	18
Metallic Cu in separator[a]	10
Cutting of separator by honeycomb current collector	9
Equipment malfunction[b]	7
Short in feedthrough	3
Quality control	2
Broken positive conductor	2
Unidentified	
Declining performance[c]	7
Short circuits	3

[a] FeS cells only.

[b] Overcharge, temperature excursion, or polarity reversal.

[c] Generally indicative of early stages of short circuit.

VII. CELL CHEMISTRY
(M. F. Roche)

The objectives of the cell chemistry studies are (1) to investigate specific chemical and electrochemical problems that arise in the development of cells and batteries, (2) to conduct studies that are expected to lead to improvements in cell design, and (3) to provide a basic understanding of the processes that occur within cells.

A. Out-of-Cell Tests of Metal Sulfide Electrodes

1. Phases in FeS_2 Electrodes
(A. E. Martin)

An earlier study (ANL-8057, p. 22) indicated that one of the intermediate phases (referred to as Z phase) in the discharge of FeS_2 electrodes had the approximate composition $Li_4Fe_2S_5$. However, this composition was recently found to be incorrect because the Z phase formed as a single-phase layer on FeS_2 particles during the first discharge of an FeS_2 electrode. This layer was at first (ANL-77-68, p. 49) treated as a new phase, but further investigations have shown that the layer was Z phase. Any single-phase product must lie on the normal composition path for discharge of the FeS_2 electrode. Thus the Z-phase composition has the empirical formula Li_yFeS_2.

Additional out-of-cell tests have now been made to establish the value of y. Mixtures of Li_2FeS_2 and FeS_2* in graphite crucibles were sealed under vacuum in quartz ampoules. The ampoules were heated to about 930°C in order to melt the sulfides, cooled rapidly to room temperature, and annealed for five days at about 475°C. The results of metallographic examinations of the products are reported in Table VII-1. X-ray diffraction examinations† were essentially in agreement with these results. However, the minor amounts of FeS_2 present in the first two samples were not detected by X ray. The W phase (samples 4, 5, and 6) coexisted with $Fe_{1-x}S$ and had a mottled structure as if it were a solid solution that had decomposed into other phases on cooling. X-ray diffraction could only identify this phase as a distorted Li_2FeS_2-type structure. A detailed study of this phase is in progress.

The minor amounts of $Fe_{1-x}S$ in the first three samples are believed to be the result of sulfur vaporization to free spaces in the ampoules. Therefore, sample 3, which is $Li_{1.5}FeS_2$ (or $Li_3Fe_2S_4$) and is essentially a single phase, is identified as a Z-phase. Equilibrium phases between FeS_2 and Li_2FeS_2 can then be represented as follows:

$$FeS_2 \rightarrow Li_3Fe_2S_4 \rightarrow \text{W phase} + Fe_{1-x}S \rightarrow Li_2FeS_2$$

The discharge of FeS_2 appears to follow this path, but the charge of FeS_2 may follow a different path according to cyclic voltammetry results (ANL-77-68, p. 48).

---

*Both compounds were metallographically pure, single-phase materials.

†B. S. Tani, Analytical Chemistry Laboratory, ANL.

Table VII-1. Products of Li_2FeS_2 and FeS_2 Reactions

Sample No.	Li_2FeS_2: FeS_2 Ratio	Empirical Formula	Major Phases	Minor Phases
1	1.50	$Li_{1.20}FeS_2$	Z	FeS_2, $Fe_{1-x}S$
2	2.00	$Li_{1.33}FeS_2$	Z	FeS_2, $Fe_{1-x}S$
3	3.00	$Li_{1.50}FeS_2$	Z	$Fe_{1-x}S$
4	4.00	$Li_{1.60}FeS_2$	$Fe_{1-x}S$, Z	W
5	5.00	$Li_{1.67}FeS_2$	$Fe_{1-x}S$, W	-
6	7.00	$Li_{1.75}FeS_2$	$Fe_{1-x}S$, W	-

2. Sulfur Vaporization Rates
(A. E. Martin)

Cyclic voltammetry results (given in the next section) showed that NiS_2 has better electrochemical reversibility than FeS_2. Thus, a comparison of sulfur vaporization rates for these two systems is of interest. Samples were prepared from mixtures of electrolyte (LiCl-KCl) and each of the following: (A) FeS_2, (B) FeS_2-Li_2S,* (C) $NiS_{1.8}$ and (D) $NiS_{1.8}$-LiS_2.* The $NiS_{1.8}$ was a mixture of NiS and NiS_2. The samples were placed in graphite crucibles (inside diameter, 1.27 cm), and were then heated at 527°C† in an open furnace well of a helium-atmosphere glovebox. Apparent sulfur/metal ratios were calculated from weight-loss measurements on the assumption that the losses were sulfur from the metal sulfide. The ratios are plotted *vs.* time of heating in Fig. VII-1.

Curves A and C show that the sulfur vaporization rate of $NiS_{1.8}$ is about a factor of three higher than that of FeS_2. Curves B and D show that vaporization rates are much higher for both sulfides after Li_2S additions.‡ The rates for both sulfides with Li_2S added are about the same. In fact, if curve D were recalculated for the NiS_2 fraction of the $NiS_{1.8}$, the resulting curve would overlay curve B for up to 60 hr of heating. After samples B and D reached sulfur-to-metal ratios of 1.75, their empirical compositions ($Li_{0.5}FeS_2$ and $Li_{0.5}NiS_2$, respectively) corresponded to metal disulfide electrodes that were partly discharged.

The above data indicate that both metal-disulfide electrodes will exhibit comparable vaporization losses. However, the electrochemical properties of NiS_2 and FeS_2 differ greatly. The electrochemical effects may drastically modify the behavior of the Li-Fe-S and Li-Ni-S systems in operating cells. Therefore, tests on engineering-scale NiS_2 cells are being conducted to determine the influence of electrochemistry on sulfur vaporization.

*Mole ratio of 4:1.

†Cell operating temperatures are about 427°C. A higher temperature is used here in order to complete the tests in a reasonable period of time.

‡This effect has been observed previously in a Li_2S-FeS_2-electrolyte mixture (ANL-77-35, p. 50).

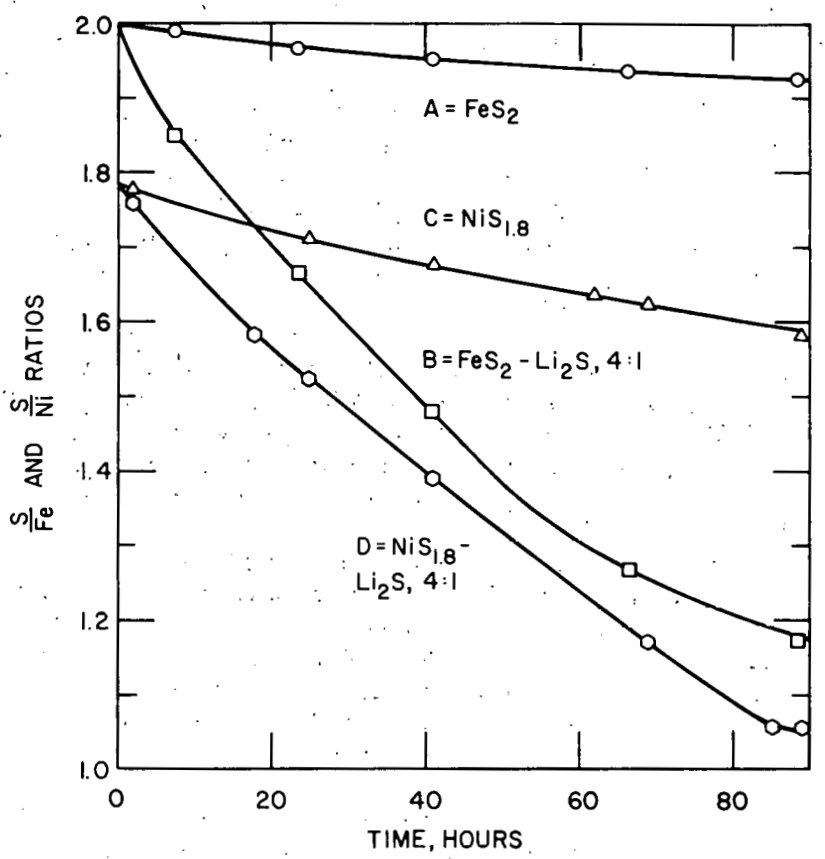

Fig. VII-1. Sulfur Losses from Li-Fe-S and Li-Ni-S Suspensions in LiCl-KCl at 527°C

B. Cyclic Voltammetry of Metal Sulfide Electrodes
(S. K. Preto, S. von Winbush,* M. F. Roche)

In ANL-77-68, pp. 46-48, the cyclic voltammetry of FeS_2 in LiCl-KCl electrolyte at 405°C was described. The voltammogram showed that the discharge of FeS_2 was not kinetically hindered. However, the charge reaction was kinetically hindered, requiring both electrochemical and chemical steps to induce formation of FeS_2. Owing to the poor charge behavior, experiments were initiated to search for electrodes having better electrochemical reversibility. The search consisted of voltammetry tests of the following electrodes: FeS_2 with additives, NiS_2 and NiS_2-FeS_2, and CoS_2. The experimental technique was the same as that used to study the FeS_2 electrode. Cyclic voltammetry was conducted at a very low scan rate (0.015-0.05 mV/sec) in LiCl-KCl electrolyte at about 407°C using LiAl (45 at. % Li) counter and reference electrodes. The working electrodes were 3-5 cm^2 in area, and contained various metal-sulfide powders (0.1 to 0.2 A-hr) in reticulated carbon foam† within a molybdenum housing.

*Visiting Professor, State University of New York, Old Westbury, NY.

†Chemotronics International, Inc., Ann Arbor, MI.

1. Additives for FeS_2 Electrodes

The majority of the additives tested for their ability to lower the voltage of the FeS_2 charge peak toward the desired value, 1.74 V (see ANL-77-68, p. 48), proved to be ineffective. These included (in mol %): TiS_2, 25; MnS, 30; MoS_2, 20; Cos_2, 15; $CuFeS_2$, 15, Cr_2S_3, 12; and Ce_2S_3, 10. Because the FeS_2 electrodes were operated in carbon foam and FeS was generated *in situ* by sulfur losses during cycling, carbon and FeS were also tested as additives, but also proved to be ineffective.

Sodium chloride (10 mol % in the electrolyte) was also tested as an additive to the LiCl-KCl electrolyte in FeS_2 cells. The effects of this additive were: (1) the NaCl shifted the charge reaction at high voltages from 1.86 to about 1.80 V (the associated discharge reaction was not shifted); and (2) the NaCl shifted charge-discharge reactions at low voltages, which are reversible and caused by formation and discharge of Li_2FeS_2, from 1.34 to 1.30 V. An unequivocal interpretation of these multiple effects is not possible at present, but voltage decreases due to sodium-ion incorporation in electroactive species that already contain lithium ions is a possibility. The only unshifted reaction was the high-voltage discharge of FeS_2; this species does not contain lithium ions. If this interpretation is correct, the reaction shifts do not represent an improvement in electrochemical reversibility, but the same undesirable reactions occurring at a slightly lower voltage.

Hastelloy B Foametal,* a Ni-Mo-Fe alloy that is used as a current collector in some FeS_2 cells, was also studied. Over 90% utilization of the theoretical capacity was achieved, but the utilization at high voltages declined with cycling. This decline is attributed to reaction of FeS_2 with Hastelloy B (ANL-77-17, p. 37). In this brief, 11-day test of Hastelloy B, no significant improvement in the position of the high-voltage reaction of FeS_2 was observed. However, postoperative examinations of engineering-scale cells have indicated that no Li_2S appears in the separators of cells that use this current collector (ANL-77-35, p. 49). This long-term beneficial effect of Hastelloy B is probably a result of its corrosion product, nickel sulfide. Nickel sulfide may inhibit sulfur losses by making FeS_2 more reversible (see next section).

2. NiS_2 and NiS_2 + FeS_2 Electrodes

Studies of the nickel sulfide electrode began with attempts to improve the reversibility of FeS_2 through additions of NiS. Additions of 12, 17, and 22 mol % NiS did not lower the voltage of the FeS_2 charge reaction to the desired voltage, 1.74 V, but a minor peak near 1.78 V, which became larger with increasing nickel content, was observed. Samples of NiS and NiS_2† were then tested. Both proved to be electrochemically reversible. The voltammogram for NiS_2 is given in Fig. VII-2. The left side of each charge peak (above the line) intercepts the voltage axis at essentially the same voltage as the right side of each corresponding discharge peak (below the line). This means the reactions

*Foametal, Inc., Willoughby, Ohio.

†Actually $NiS_{1.8}$ according to assay by W. E. Streets, Analytical Chemistry Laboratory.

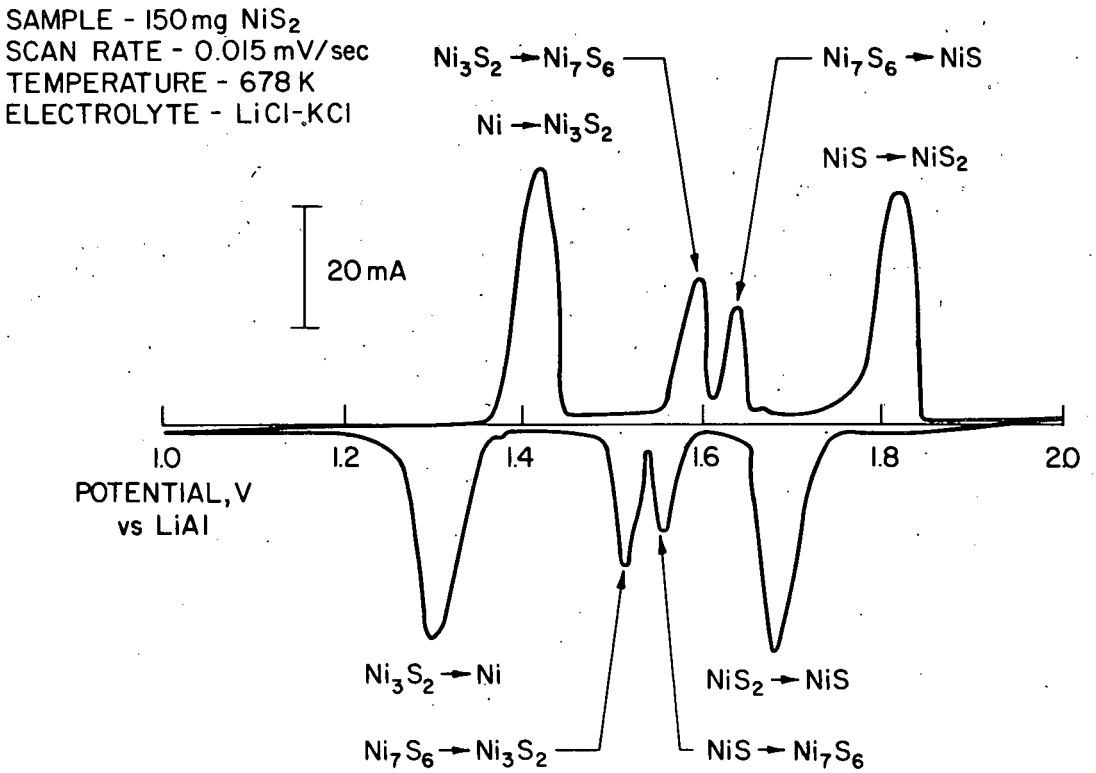

Fig. VII-2. NiS_2 Voltammogram

are electrochemically reversible. The compound Ni_7S_6 is not well characterized thermodynamically, but the experimental emfs *vs.* LiAl for Ni, Ni_3S_2 (1.36 V) and for NiS, NiS_2 (1.74 V) agree well with thermodynamic values of 1.362 and 1.727 V, respectively (ANL-77-17, p. 50).

The good reversibility of NiS_2 alone prompted an additional test of the Ni-Fe-S system. A voltammogram for an equimolar mixture of NiS_2 and FeS_2 is shown in Fig. VII-3. This mixture had adequate reversibility (poorer than NiS_2 alone, but much better than FeS_2). As a result of these tests, engineering-scale studies of Li-Al/NiS_2 and Li-Al/NiS_2-FeS_2 (equimolar) cells have been initiated.

3. CoS_2 Electrode

Cobalt disulfide was of interest because it is employed as an additive in FeS_2 and NiS_2 electrodes (see Cell R-31 in Appendix A). The CoS_2 electrode gave voltammetry peaks associated with formation and discharge of Co_9S_8, Co_3S_4, and CoS_2. As can be seen below, reversibility improved with decreasing voltage. The potentials (in V *vs.* LiAl) at which reactions began were as follows:

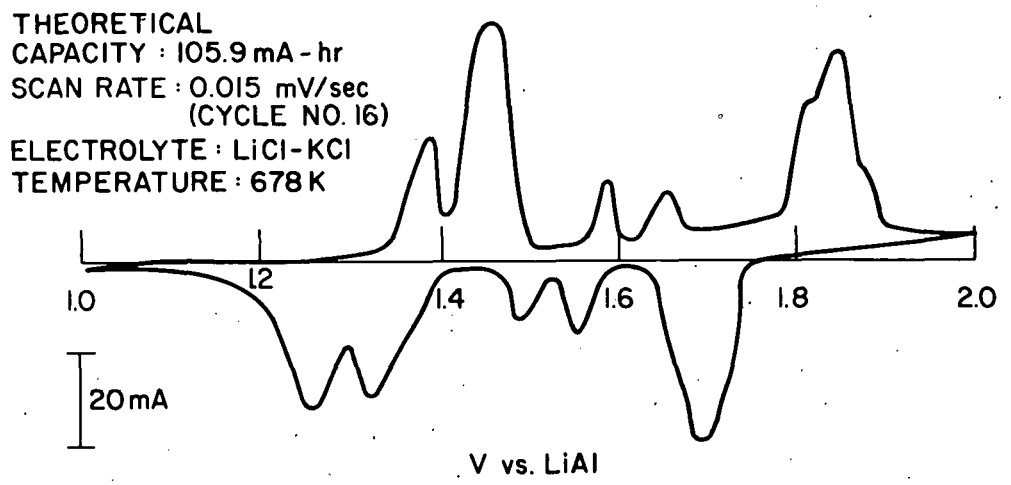

Fig. VII-3. Voltammogram for Equimolar Mixture of NiS_2 and FeS_2

$CoS_2 \rightarrow Co_3S_4$	1.72	0.08 V difference
$Co_3S_4 \rightarrow CoS_2$	1.80	
$Co_3S_4 \rightarrow Co_9S_8$	1.62	0.06 V difference
$Co_9S_8 \rightarrow Co_3S_4$	1.68	
$Co_9S_8 \rightarrow Co$	1.34	0.04 V difference
$Co \rightarrow Co_9S_8$	1.38	

Comparing voltammograms, we conclude that FeS_2 (0.12 V difference) is less reversible than CoS_2, and that CoS_2 is less reversible than NiS_2. Thus, reversibility of disulfides improves with increasing atomic number within the transition metal triad: Fe, Co, Ni.

C. Tests of Metal Sulfide Cells

These are relatively short-term tests designed to assess the performance and chemistry of various electrode mixtures. Tests of iron sulfide, nickel sulfide, and titanium sulfide electrodes were conducted in this period.

1. Cells with Iron Sulfide Electrodes

(K. E. Anderson, C. Hickson,* D. R. Vissers)

Lithium-aluminum/iron disulfide cells with capacities of about 5 A-hr were operated in LiCl-KCl electrolyte at approximately 430°C to discover additives that improve the electrochemical reversibility of FeS_2. The Li-Al was contained in a stainless steel housing with an area of 15 cm^2 and an iron Retimet current collector; the metal sulfide [FeS_2, $Fe(Mo)S_2$, or $Fe(Ag)S_2$] was contained in a carbon housing with an area of about 10 cm^2 and a molybdenum-screen current collector. The FeS_2 electrodes using Ag_2S (33 mol %) and MoS_2

*Student Aide, Georgia Tech.

(4.5 mol %) additives had voltage curves similar to those of normal Li-Al/FeS_2 cells; thus, no improvement in electroreversibility was detected for these additives.

In the above experiments, two Li-Al (7.4 A-hr)/FeS_2 (4.63 A-hr) cells were operated that employed LiCl-KCl electrolyte from different suppliers. One of these cells yielded only one third of its theoretical capacity, whereas the other cell operated at essentially full capacity. The latter cell exhibited the poor electroreversibility described in recent voltammetry studies (ANL-77-68, p. 48), but the former cell, which operated only on the highest voltage plateau of the LiAl/FeS_2 couple, had excellent electrochemical reversibility. The average charge voltage was 1.80 V and the average discharge voltage was 1.72 V (both at a current density of 10 mA/cm^2). It is believed that full utilization was somehow inhibited in this cell by an off-eutectic electrolyte composition. Electrolyte assays are now in progress.

As a result of these cell tests, additional cyclic voltammetry studies of FeS_2 were conducted. These studies (to be described more fully in a later report) confirmed that the high-voltage reaction, $2FeS_2 + 3\ Li \rightleftarrows Li_3Fe_2S_4$, is reversible in LiCl-KCl electrolyte if the electrode is prevented from discharging to lower-voltage compounds. From these tests, the electrochemical irreversibility of FeS_2 has been identified as resulting from compounds present between 37.5 and 50% utilization of FeS_2 during discharge.

2. Cells with Nickel Sulfide Electrodes
(Z. Tomczuk, A. E. Martin, A. Johnson,* J. D. Arntzen, D. R. Vissers)

Four LiAl (2 A-hr)/LiCl-KCl/NiS_2 (1 A-hr) cells were operated at 430°C to test the effects of various additives on NiS_2 electrode performance. The LiAl electrodes had stainless steel housings, and the NiS_2 electrodes had carbon housings (area, 5 cm^2). Two of the NiS_2 electrodes contained 10 mol % CoS_2, one contained about 1 g graphite powder, and one had no additives. Only the electrode with graphite performed well (similarly constructed FeS_2 cells perform well with no additive); its utilization was 82% for current densities of 20 to 60 mA/cm^2. Thus, carbon is a good current collector for NiS_2 electrodes. The cell with no additives had poor utilization. The cells with CoS_2 additive exhibited irregular discharge-voltage curves (sharp declines in voltages and a later recovery to the normal voltage). This pattern duplicated the behavior of a recent engineering-scale cell (R-31).

An engineering-scale LiAl/NiS_2 cell with a theoretical capacity of 75 A-hr was constructed. This cell employed a molybdenum sheet as the current collector in the positive electrode. The cell exhibited irregular voltage curves similar to those of the LiAl/Ni(Co)S_2 cell, and has not yet performed well at high currents. Its capacity after 17 cycles is about 50 A-hr at 3 A currents. Cycling is continuing to determine whether the cell performance will improve.

---

*Undergraduate Summer Research Participant, Albany State College, Albany, GA.

3. Cells with Titanium Sulfide Electrodes

(J. D. Arntzen, D. R. Vissers, K. E. Anderson, A. Johnson,* Z. Tomczuk)

An engineering-scale LiAl/TiS_2 cell (theoretical capacity, 125 A-hr) was fabricated by Eagle-Picher Industries using their Li-Al/FeS_2 cell hardware. This cell, like an earlier (75 A-hr) TiS_2 cell (ANL-77-68, p. 51), failed in <20 cycles of operation. The cell operation was conservative; the temperature was 400°C and the cutoff voltages were 1.2 V on discharge and 2.1 V on charge. Nevertheless, the coulombic efficiency had declined to about 50% by cycle 18. Postoperative examinations† have indicated that the short circuits in these two cells may have been due to mechanical problems. In the 75 A-hr cell, a metallic-appearing phase developed at the top of the cell, and in the 125 A-hr cell the BN fabric separator was cut by the positive-electrode frame. No Li_2S or titanium-containing species were found in the separators of these two cells. Additional engineering-scale work is warranted; designs that will avoid the above problems are now being developed.

The power capabilities of TiS_2 were evaluated in a Li/TiS_2 cell having a design identical to that used earlier to evaluate the FeS_2 electrode.[2] The positive electrode disk (2.38 cm dia., 0.4 cm thick) contained 3.75 g of TiS_2 (66% theoretical density) and was held in a graphite housing. This cell was operated in LiCl-KCl electrolyte at temperatures of 380, 430, and 460°C. The peak power densities (15-sec pulses) were about 0.40, 0.47, and 0.55 W/cm^2, respectively. These values compare favorably with the earlier results for FeS_2, which had a peak power density of about 0.5 W/cm^2 over this temperature range.

The following modifiers‡ for TiS_2 were tested in cells: chromium ($Cr_{0.05}Ti_{0.95}S_2$ and $Cr_{0.25}Ti_{0.75}S_2$), molybdenum ($Mo_{0.05}Ti_{0.9}S_2$ and $Mo_{0.25}Ti_{0.75}S_2$), and copper ($Cu_{0.5}TiS_2$). These cells had LiAl negative electrodes with theoretical capacities of 2 A-hr, and were operated at temperatures of about 430°C. The theoretical capacity of the positive electrode was calculated by assuming that the reaction products would contain 0.5 mole of lithium per mole of sulfur (as in $LiTiS_2$). With the exception of $Cu_{0.5}TiS_2$, which had a single discharge plateau at 1.65 V, the materials exhibited a voltage decline with state of discharge similar to that of TiS_2 (ANL-76-98, p. 52). The electrodes that exhibited the best performance were $Cu_{0.5}TiS_2$ (80% utilization at a current density of 26 mA/cm^2) and $Mo_{0.05}Ti_{0.9}S_2$ (80% utilization at 13 mA/cm^2). However, none of these materials appeared to offer any advantages over TiS_2 alone, which has very good performance characteristics (ANL-76-98, p. 52).

4. Lithium Wick/FeS Cells

(L. E. Ross, M. F. Roche)

A cylindrical Li wick/FeS cell with an 86 A-hr theoretical capacity was tested in earlier studies (ANL-77-17, p. 48). This cell was operated for

---

*Undergraduate Summer Research Participant, Albany State College, Albany, GA.

†F. C. Mrazek and J. E. Battles, Materials Group.

‡Compounds prepared by Electrochemical Corp., Mountain View, CA.

72 cycles before operation was voluntarily terminated. The present study consists of the design and testing of a prismatic Li wick/FeS cell.

The cell wick was made from a 100-mesh stainless steel screen (100 cm long and 11.2 cm wide) which had 0.3-cm-deep pleats perpendicular to its length; this pleating reduced the length of the wick to about 20 cm. The wick was spot welded around the inner surface of a stainless steel can (3.1 cm thick, 8.2 cm wide, and 14.0 cm deep). This assembly was placed in a furnace well at 400°C, and the electrolyte, LiCl-KCl plus 4.2 mol % LiF, was added. A Li-1.2 at. % Cu alloy was then added incrementally until 78 A-hr of lithium was stored in the pleats of the wick. The liquid volume was adjusted to permit about 1 cm of the pleated wick to remain above the electrolyte during cell operation.

The positive electrode contained 13 log-shaped units of iron Retimet (0.7 × 1.1 × 5.9 cm), each of which was wrapped in a 325-mesh stainless steel screen. A total of 114.6 g of FeS was loaded into the iron Retimet units; this is equivalent to a theoretical capacity of 70 A-hr. The iron Retimet units were stacked on top of each other within a picture frame housing, and were tack-welded in place. The housing faces were covered by a 40-mesh stainless steel screen and a ZrO_2 cloth retainer. The positive electrode was attached to a cell cover, by means of a standard feedthrough, and lowered into the cell. The assembled cell weighed 1.01 kg.

The cell, which short-circuited after 11 cycles of operation, achieved specific energies of more than 70 W-hr/kg at low rates (2-A charges, 1-A discharges). The failure was caused by shifting of the positive electrode units. This shifting caused the thickness of the positive electrode to increase, thereby bringing it into contact with the wick.

5. Cells with Nonswelling FeS Electrodes

(K. E. Anderson, J. D. Arntzen,* P. F. Eshman,* D. R. Vissers)

As a result of the above experiments, studies have been initiated on nonswelling FeS electrodes for prismatic cells. A modular design was selected for the positive electrode.

For a preliminary test, two iron modules having iron Retimet current collectors (0.7 cm thick) and ZrO_2 cloth retainers were fabricated. The face of each module was a flat picture frame to which two 16-mesh iron screens were welded. (The two screens were slipped into a tray, and the picture frame was then welded to the tray to form the rectangular module.) One module was loaded with LiAl and the other with FeS. The FeS module contained 1.65 g of Fe, 1.36 g of Li_2S, and 6.55 g of FeS (total capacity, 5.5 A-hr) and the Li-Al module contained 6 g of LiAl and 3 g of Al (total capacity, 7.7 A-hr). A BN cloth on the FeS electrode served as the cell separator. The cell operated for 15 cycles during which time as much as 70% of the active material was utilized. Post-test examination by the Materials Group indicated no swelling of either electrode module. Thus the modular design of the FeS electrode has potential for use in the fabrication of an FeS cell such as the lithium wick/FeS cell. Engineering-scale cells will be fabricated. The design of the FeS electrode in this type of cell might contain 10 rectangular modules (5 × 2.5 × 0.9 cm) on each electrode side.

*Industrial Cell and Battery Testing Group at ANL.

VIII. ADVANCED BATTERY RESEARCH
(M. F. Roche)

The objective of this work is to develop new secondary cells that use inexpensive, abundant materials. The experimental work ranges from cyclic voltammetry studies and preliminary cell tests through the construction and operation of engineering-scale cells for the most promising systems. The studies at present are focused on the development of new cells with molten-salt electrolytes. During this quarter, the studies consisted of cycling tests of alkaline-earth/metal-sulfide cells.

A. Testing of Calcium Cells

A Ca-Mg-Si negative electrode has been developed that performs almost as well as Li-Al negative electrodes (ANL-77-17, p. 52 and ANL-77-35, p. 53). However, attempts to develop a suitable positive electrode for the calcium cells have been frustrated by two problems. (1) Positive electrodes of FeS cannot be used in large-scale calcium cells because iron is oxidized to $FeCl_2$ (ANL-77-35, p. 59). This problem has also occurred in Li-Al/FeS_2 cells, but to a lesser extent (ANL-77-68, p. 46). (2) Reasonable utilization of metal-sulfide electrodes in cells with capacities of 5 to 10 A-hr has been achieved, but much lower utilizations are achieved in cells with capacities of about 100 A-hr (ANL-77-68, p. 51, ANL-77-35, p. 39). The first problem was easily solved. Nickel, for example, is more resistant to oxidation than iron; thus the nickel sulfides are more suitable electrodes for these cells (ANL-77-68, p. 52). The second problem has not been solved yet, and future studies of calcium cells will focus on solutions to this problem.

1. Tests of Small-Scale Calcium Cells
(L. E. Ross, S. M. Faist*)

During this quarter, tests of Fe-Ti-S and NiS_2 positive electrodes in calcium cells were conducted. These tests were not directed toward solving the above scale-up problem, but were preliminary assessments of alternative positive electrodes.

The Fe-Ti-S electrode was tested in a $CaAl_2$-Al (5.3 A-hr)/Fe-Ti-S (1 A-hr) cell at 500°C. The positive electrode was uncharged, had a current collector of carbon foam, and was held in a graphite housing with an area of 5 cm^2. The amounts of Fe, Ti, and CaS added to the positive electrode were based on the assumption that Fe_2TiS_4, a sulfospinel, would form at full charge. The negative electrode was half-charged, and had an area of 15 cm^2. The electrolyte in this cell consisted of LiCl (55 mol %)-KCl (14 mol %)-$CaCl_2$ (31 mol %). The cell performed well. The positive-electrode utilization was 75% at a current density of 20 mA/cm^2 and 70% at 40 mA/cm^2 with charge and discharge cutoff voltages of 2.05 and 1.00 V, respectively. The coulombic efficiency of the cell was 97%. This cell had two voltage plateaus, one at an emf of 1.63 V (one fourth of theoretical capacity during discharge) and the other at 1.39 V (three fourths of theoretical capacity during discharge). Analysis of the charged electrode† identified $Fe_{0.6}Ti_{0.4}S$ as the major phase and $FeTi_{1.35}S_{3.12}$

*Resident Student Associate, Massachusetts Institute of Technology.

†X-ray diffraction by B. S. Tani, Analytical Chemistry Laboratory, ANL.

as a minor phase. Both these products were richer in titanium than the starting mixture, thus indicating that some adjustments are needed to arrive at a practical system. At present, whether or not the Fe-Ti-S system will operate well on an engineering scale is not known; the major concern is the ability of the system to resist oxidation to $FeCl_2$ in solution.

Two nickel disulfide cells having positive-electrode capacities of 1 A-hr (5 cm^2 area) and 5 A-hr (15 cm^2 area) were operated at 442°C in LiCl-KCl (eutectic) plus 8 mol % $CaCl_2$. The negative electrodes ($CaAl_2$) had capacities and areas about four times as large as those for the positive electrodes. The positive electrode mixtures included cobalt (7 wt % of the metal). The positive electrodes had current collectors of carbon foam, and were contained in graphite housings. The charge and discharge cutoff voltages of this cell were 2.2 and 1 V, respectively. The positive-electrode utilizations at current densities of 20 mA/cm^2 were about 50% in the smaller cell and 70% in the larger cell. As determined in ANL-77-68, p. 52, the percent utilization of the monosulfide, NiS, was somewhat higher than that for NiS_2, but additional tests are needed to determine which sulfide will perform best in large-scale cells.

2. Test of Large-Scale Calcium Cell
(J. D. Arntzen, K. E. Anderson, D. R. Vissers)

A prismatic, uncharged Mg_2Si/Ni-CaS cell with a theoretical capacity of 90 A-hr was operated for 76 cycles before cell operation was voluntarily terminated. The electrolyte was LiCl-KCl (eutectic) plus 8 mol % $CaCl_2$. The positive-electrode mixture, which contained 20% more CaS than required for NiS formation, was hot-pressed onto a central current-collector sheet of molybdenum. The two negative electrodes contained iron Retimet current collectors. A particle retainer of ZrO_2 cloth was used for the positive electrode and ZrO_2 cloth and 325-mesh stainless steel screens for the negative electrodes. The separator was BN fabric. The coulombic efficiency of the cell was satisfactory (about 90%). At currents of 3 A (10 mA/cm^2) and 10 A, the capacity was 33 A-hr and 27 A-hr, respectively. Increasing the charge cutoff voltages from 2.1-2.2 V to as high as 2.7 V during 5-A currents increased the capacity only to 37 A-hr. Other unsuccessful attempts to increase the capacity included raising the temperature from 450 to 500°C and trickle charging. A NiS_2 reference electrode situated in the electrolyte above the electrodes indicated that the positive electrode was polarizing rapidly toward the end of charge. Thus, the positive electrode was limiting cell performance. A distributed current collector (carbon fibers) will be tried in the positive electrode of the next cell in this series to determine whether cell performance is limited by poor current collection.

B. Testing of Magnesium Cells

1. Tests of Nickel Sulfide Positive Electrodes
(C. C. Sy, Z. Tomczuk)

Two Mg_2Cu (5 A-hr)/nickel sulfide (1 A-hr) cells were operated in NaCl-KCl-$MgCl_2$ electrolyte. The nickel sulfide electrodes were contained in 5-cm^2 graphite housings and 1 g of powdered graphite was added for current collection. The Mg_2Cu electrodes (15 cm^2 area) had iron Retimet current collectors and stainless steel housings. One of the cells employed a NiS positive electrode and was operated at 500°C. Its utilization, using a

charge cutoff of 1.56 V and a discharge cutoff of 1.0 V, was 66% at a current density of 11 mA/cm^2 and 45% at 18 mA/cm^2. The other cell had a NiS_2 positive electrode and was operated at 450°C. Its utilization, using cutoffs of 2.0 and 1.0 V, was 70% at a current density of 6 mA/cm^2 and 65% at 17 mA/cm^2. Thus, neither electrode achieved very high utilization. Tests will be conducted to further define the capabilities and limitations of the nickel sulfide electrode in magnesium cells.

2. Test of Mg_2Al_3 Negative Electrode
(K. E. Anderson, D. R. Vissers)

The performance of Mg_2Al_3 was evaluated at 445°C in a Mg_2Al_3/NaCl-KCl-$MgCl_2$/Al cell, which was operated with cutoff voltages of ±0.38 V. Iron Retimet current collectors were employed in both electrodes, and they were covered with layers of ZrO_2 cloth and a stainless steel screen. The Mg_2Al_3 electrode had a capacity of 1.65 A-hr and an area of 4.6 cm^2; the Al electrode had a capacity of 7.3 A-hr (as Mg_2Al_3) and an area of 15.6 cm^2. The coulombic efficiency of the cell exceeded 95% for the first 49 cycles, but decreased to 80% by cycle 51. In an examination of the smaller electrode, large hexagonal crystals of magnesium metal were found on the stainless steel screen. This suggests that screens should be avoided when fabricating cells of this type.

The performance of the electrode material was poor. At a current density of 11 mA/cm^2 (based on the area of the small electrode), the utilization was 44%. Increasing the current density on discharge to 44 mA/cm^2 led to a utilization of only 17.1%.

REFERENCES

1. J. M. Smith, *High Temperature Materials and Technology*, E. M. Sherwood, I. E. Campbell, Eds., John Wiley & Sons, Inc., New York, p. 142 (1967).

2. D. R. Vissers, Z. Tomczuk, R. K. Steunenberg, J. Electrochem. Soc. *121*, 665 (1974).

THIS PAGE

WAS INTENTIONALLY

LEFT BLANK

APPENDIX A.

SUMMARY OF LARGE-SCALE CELL TESTS

APPENDIX A. Summary of Large-Scale Cell Tests

Cell Description[a]	Max. Performance @ Indicated Rate[b] A-hr	W-hr	Rates, hr Disch.	Charge	Initial Eff.,[c] % A-hr	W-hr	Life Characteristics Days[d]	Cycles[d]	% Decline in[e] Capacity	Energy	A-hr Eff.	W-hr Eff.	Remarks
2B8, Li-Al/FeS_2-CoS_2, C, S, 149/149, 13.5 × 15.6 × 3.8 cm, 1.900 kg	118 117	159 157	11.8 9.0	11.8 9.0	99	82	378	533	39	41	16	23	Start-up and operation with cell blanketed in Kaowool insulation, exposed to air.
I-3-B-1, Li-Al/FeS-Cu_2S, C, S, 170/127, 13.5 × 15.6 × 3.8 cm, 2.035 kg	101 88 76 68	131 108 92 73	10 5.9 3.8 2.7	10 5.9 3.8 2.7	99	81	235	>406	6	8	7	8.5	EP cell, with slightly thinner positive and slightly denser negative. 67 W-hr/kg at 10-hr rate.
I-3-B-2, Li-Al/FeS-Cu_2S, C, S, 170/127, 13.5 × 15.6 × 3.8 cm, 2.07 kg	69 85	85 104	7 8.5	7 8.5	99	82	>33	>43	0	0	0	0	Previously qualification tested (42 days, 48 cycles). Now in check-out of new furnace and minicycler equipment.
I-3-C-2, Li-Al/FeS-Cu_2S, C, S, 193/145, 13.5 × 15.6 × 3.8 cm (shimmed cell), 1.79 kg	97	112	10	10	98	84	>132	>250	36	32	0	1	EP cell, 4.2 mm thick positive electrode. 63 W-hr/kg at 10-hr rate. Constant current compared to constant voltage charge.
I-4-1, Li-Al/FeS_2-CoS_2, C, S, 170/156, 13.5 × 15.6 × 3.8 cm, 2.18 kg	108	151	11	11	99	83	39	42	31	33	25	44	EP (thick) FeS_2 cell with offset positive terminal rod. Terminated, declining performance.
I-4-2, Li-Al/FeS_2-CoS_2, C, S, 170/156, 13.5 × 15.6 × 3.8 cm, 2.21 kg	108 81	150 108	10.8 5.4	10.8 5.4	99	77	68	121	40	40	74	75	EP (thick) FeS_2 cell with offset positive terminal rod. Terminated, poor efficiency and capacity.
I-4-3, Li-Al/FeS_2-CoS_2, C, S, 170/156, 13.5 × 15.6 × 3.8 cm, 2.16 kg	85 76	119 102	8.5 5.0	8.5 5.0	99	75	55	91	22	28	4	8	EP (thick) FeS_2 cell with offset positive terminal rod. Terminated, will not accept charge.
I-6-A-1, Li-Al/FeS_2-CoS_2, C, S, 199/156, 13.5 × 15.6 × 3.2 cm, 1.66 kg	97	133	10	10	99	82	85	109	15	12	22	18	More compact EP FeS_2 cell, with thinner, less porous electrode (positive). 55 at. % Li-Al. 72 W-hr/kg at 4-hr rate, peak power 57 W/kg. Terminated, low coulombic efficiency.

(contd)

APPENDIX A. Summary of Large-Scale Cell Tests

Cell Description[a]	Max. Performance @ Indicated Rate[b] A-hr	W-hr	Rates, hr Disch.	Charge	Initial Eff.,[c] % A-hr	W-hr	Life Characteristics Days[d]	Cycles[d]	% Decline in[e] Capacity	Energy	A-hr Eff.	W-hr Eff.	Remarks
I-6-A-2, Li-Al/FeS_2-CoS_2, C, S, 199/156, 13.5 × 15.6 × 3.2 cm, 1.66 kg	97	133	10	10	99	82	99	105	8	18	17	18	More compact EP FeS_2 cell, with thinner, less porous electrode (positive). 55 at. % Li-Al. 72 W-hr/kg at 4-hr rate, peak power 57 W/kg. Terminated, low coulombic efficiency.
I-6-B-1, Li-Al/FeS_2-CoS_2, C, S, 199/156, 13.5 × 15.6 × 3.2 cm 1.61 kg	104	146	10	10	96	80	>81	>99	20	22	7	12	More compact EP FeS_2 cell, with thinner, less porous electrode (positive). 55 at. % Li-Al and ZrO_2 retainer cloth removed from negative electrode. 75 W-hr/kg at 4-hr rate.
I-6-B-2, Li-Al/FeS_2-CoS_2, C, S, 199/155, 13.5 × 15.6 × 3.2 cm, 1.61 kg	102	146	10	10	97	80	>11	>9	0	0	0	0	Similar in design to I-6-B-1 cell, except Mo screen added to positive electrode. Cell now being qualification tested.
I-7-1, Li-Al/FeS_2-CoS_2, C, S, 230/222, 13.5 × 15.6 × 3.8 cm, 1.95 kg	95 80	120 99	9.5 5	9.5 5	92	74	>26	>41	0	0	0	0	Compact EP one piece positive shimmed cell. Flexible Mo positive connection.
I-9-3, Li-Al/FeS_2-CoS_2, C, S, 106/156, 13.5 × 15.6 × 2.61 cm, 1.38 kg	59	91	10	10	96	78	>7	>17	0	0	0	0	First upper plateau cell built by EP. Yet to be qualification checked.
2B-Fe-1, Li-Al/FeS_2-CoS_2, C, S, 150/150, 13.5 × 15.6 × 3.8 cm, 1.88 kg	115	158	11	11	99	81	29	27	15	15	15	14	Baseline EP thick FeS_2 cell with Fe added to face of positive electrode. Terminated, decline in performance.
I-04-008A, Li-Al/FeS_2-CoS_2, C, S, 211/158, 14.02 × 21.0 × 3.2 cm, 2.488 kg	125	188	12	12	97	77	31	130	12	13	11	10	Gould, FeS_2 upper-plateau cell. Part of cell test matrix. Terminated, cell short-circuited.

(contd)

APPENDIX A. Summary of Large-Scale Cell Tests

Cell Description[a]	Max. Performance @ Indicated Rate[b] A-hr	W-hr	Rates, hr Disch.	Charge	Initial Eff.,[c] % A-hr	W-hr	Life Characteristics Days[d]	Cycles[d]	% Decline in[e] Capacity	Energy	A-hr Eff.	W-hr Eff.	Remarks
PFC-1-01, Li-Al/FeS_2-CoS_2, C, O, 150/133, 13.5 × 15.6 × 3.9 cm, 2 kg	101	138	10	10	98	77	64	54	25	23	12	10	First pellet cell with FeS_2 positive. Difficulties welding heavy bus in positive grid. Terminated, decline in A-hr eff.
PFC-3-01, Li-Al/FeS_2-CoS_2, C, O, 150/159, 13.5 × 15.6 × 3.8 cm, 1.92 kg	106	133	10	10	98	66	>21	>26	8	9	2	2	First pellet cell built with no center plate in positive. Cell has high resistance thought to be due to broken Mo rod-electrode weld.
PC-1-01, Li-Al/FeS-Cu_2S, C, O, 150/136, 5.30 in. × 6.15 in. × 1.48 in., 2.05 kg with allowance for cover	190 64	110	9.0 2.5	9.0 6.4	99	86	102	137	0	0	0	0	Test of pellet FeS cell concept for making large electrodes. Lowered resistance of cell. Peak specific power 45 W/kg. Cell terminated, now on standby to make room for next test.
R-29, Li-Al/FeS_2-CoS_2, U, S, 125/137, 12.7 × 12.7 × 3.5 cm, 1.55 kg	74 79 70 63	104 123 90 72	6 10 4 2	10 10 7 7	99	73	96	180	46	52	66	62	Upper-plateau cell assembled uncharged. Negative electrode is pressed Al wire, partially charged with Li-Al plaque; positive electrode, hot-pressed. Temporarily terminated.
R-30, Li-Al/FeS_2-CoS_2, U, S, 157/122, 13.3 × 15.2 × 3.5 cm, 2.19 kg	101 107 103 93 84	155 149 130 114 97	10 5 3.5 2.5 1.5	10 10 10 10 10	100	83	48	70	0	0	0	0	Upper-plateau cell. Negative electrode pressed Al-wire with excess Li. Positive electrode with high conductivity carbon additive, hot-pressed. Positive current collector with Hastelloy B screen welded to Mo sheet to provide sulfur-to-metal ratio of 1.75. Terminated.
R-31, Li-Al/NiS_2-CoS_2, U, S, 159/132, 13.3 × 15.2 × 3.5 cm, 1.88 kg	83	108	8	8	100	81	>45	>71	0	0	0	0	Four-plateau NiS_2 cell, assembled semicharged with hot-pressed NiS positive. Negative electrode pressed Al wire, partially charged with Li foil.

(contd)

APPENDIX A. Summary of Large-Scale Cell Tests

Cell Description[a]	Max. Performance @ Indicated Rate[b] A-hr	W-hr	Rates, hr Disch.	Charge	Initial Eff.,[c] % A-hr	W-hr	Life Characteristics Days[d]	Cycles[d]	% Decline in[e] Capacity	Energy	A-hr Eff.	W-hr Eff.	Remarks
R-32, Li-Al/NiS_2, U, S, 165/127, 13.3 × 15.2 × 3.5 cm, 1.90 kg	85	124	8	8	100	80	>14	>20	0	0	0	0	Same as R-31, except that heat-treated carbon was added to the positive electrode.
VB-3, LiAl/FeS_2, U, S, 146/118, 12.7 × 12.7 × 3.2 cm, 1.85 kg	65 57 55 46	97 80 67 44	6 4 2 1	12 8 8 8	97	76	>125	>255	34	31	67	66	Upper-plateau, uncharged cell completely assembled in air. Negative electrode, pressed Al wire, partially charged with Li-Al plaque. Positive electrode hot-pressed X-phase.
M-3, Li-Al/FeS_2-CoS_2, C, S, 103/74, 13.3 × 13.6 × 2.4 cm, 1.35 kg	60 73 71	82 110 112	2 5 10	8.5 10 8	98	78	57	93	25	31	28	33	Hot-pressed electrodes. Alloy is 55 at. % Li. Hastelloy B on positive replaced by Mo. Welded Mo terminal current collector connection. 4.2-6.2 mΩ resistance. Specific energy at 2-hr, and 5-hr rate is same (83 W-hr/kg). Lifetime cycling at 5-hr rate (14 A). Terminated.
M-4, LiAl/FeS_2-NiS-Mo-Fe, C, S, 165/267, 13.3 × 13.3 × 3.3 cm, 1.8 kg	135 144	187 208	9 18	9 18	97	81	>25	>36	0	0	0	0	EP cold-pressed negative/hot-pressed positive (in-house). Y_2O_3 felt separator/retainer. 3.0-4.2 mΩ cell resistance.
KK-11, Li-Al/FeS_2-CoS_2, C, S, 100/75, 13.3 × 13.6 × 2.4 cm, 1.4 kg	71	105	5	7	99	83	120	223	11	17	8	8	Carbon-bonded FeS_2-CoS_2 and 55 at. % LiAl hot pressed electrodes. Welded Mo current collector. 3.5 mΩ cell resistance. Y_2O_3 felt separator/retainer. Specific energy of 75 W-hr/kg at 5-hr rate, power density of 180 W/kg. After cycle 200, capacity remained stable at ~60 A-hr up to 150 mA/cm^2 (42 A). Voluntary termination to determine reasons for its extended lifetime with good performance in comparison to Cell M-3.

(contd)

APPENDIX A. Summary of Large-Scale Cell Tests

Cell Description[a]	Max. Performance @ Indicated Rate[b] A-hr	W-hr	Rates, hr Disch.	Charge	Initial Eff.,[c] % A-hr	W-hr	Life Characteristics Days[d]	Cycles[d]	% Decline in[e] Capacity	Energy	A-hr Eff.	W-hr Eff.	Remarks
KK-12, Li-Al/FeS_2-CoS_2-TiS_2, C, S, 150/95, 13.3 × 12.4 × 3.5 cm, 1.8 kg	90	126	8	10	98	81	>30	>40	0	0	0	0	Carbon-bonded FeS_2-CoS_2 with facial TiS_2 layer and hot-pressed LiAl (EP) electrodes. Y_2O_3 felt separator. After start-up problems, cell rebuilt with BN-felt separator.
CE-1, Li-Al/CuFeS_2, C, O, 148/147, 8.3 × 15.9 × 4.4cm	67	72	5	5	98	67	552	1006	36	34	1	0	Carbon-bonded positive/hot-pressed negative. 13 mΩ resistance. Terminated.
FM-0, LiAl/FeS-Cu_2S, C, S, 85/70, 13.0 × 15.2 × 2.5 cm, 1.67 kg	52	65	6	6	99	85	136	263	6	6	2	0	EP cold-pressed positive/iron Retimet Li-Al negative. Baseline cell. 6.5 mΩ resistance. Terminated.
FM-4, LiAl-5 wt % Zn/FeS-Cu_2S, C, S, 85/70, 13.0 × 15.2 × 2.5 cm, 1 kg	51	63	6	7	81	69	>40	>70	4	4	0	0	EP cold-pressed positive/Li-Al-Zn in iron Retimet negative. 7.3 mΩ resistance.
FM2-0, LiAl/FeS_2-CoS_2, C, S, 85/77.5, 13.3 × 15.6 × 3.2 cm, 1.75 kg	55 58	76 88	2 5	8 8	97	77	62	116	22	25	3	13	Eagle-Picher cold-pressed positive/ LiAl iron Retimet negative. Baseline cell. Upper-plateau (77.5 A-hr) operation. 7.1-7.5 mΩ resistance. Broken positive lead. Terminated.
FM2-1, LiAl-8.6 wt % Sn/FeS_2-CoS_2, C, S, 86/77.5, 13.3 × 15.6 × 3.2 cm, 1.75 kg	62 61	86 93	2 5	8 8	97	74	>104	>182	30	34	4	0	EP cold-pressed positive/Li-Al-Sn in iron Retimet negative. Upper-plateau operation. Cell resistance 7.8 mΩ.

(contd)

APPENDIX A. Summary of Large-Scale Cell Tests

Cell Description[a]	Max. Performance @ Indicated Rate[b] A-hr	W-hr	Rates, hr Dischr.	Charge	Initial Eff.,[c] % A-hr	W-hr	Life Characteristics Days[d]	Cycles[d]	% Decline in[e] Capacity	Energy	A-hr Eff.	W-hr Eff.	Remarks
PW-2, Li-Al/FeS_2-CoS_2, U, S, 180/112, 12.4 × 13.0 × 2.8 cm, 1.43 kg	92 65	148 100	18.5 6	18.5 12	∿99	73.8	36	50	54	54	64	60	Y_2O_3-powder separator. Hot-pressed Li_2S-FeS-CoS (10 wt %) positive/hot-pressed Li-Al negative. LiAl alloy is 50 at. % Li. Welded Mo sheet-terminal current collector. Fe honeycomb in negative for current collection. Powder separator + electrolyte premixed at electrolyte melting temperature. Totally sealed cell. Upper plateau, 6-10 mΩ IR. Terminated.
PW-3, LiAl/FeS_2-CoS_2, U, S, 180/120, 12.4 × 13.0 × 2.8 cm, 1.35 kg	55	86	5	8	∿99	82	34	69	43	44	68	55	MgO powder separator. Hot-pressed Li_2S-FeS-CoS (10 wt %) negative. Fe honeycomb current collector in negative electrode. Powder separator + electrolyte premixed at melting temperature of electrolyte. Totally sealed cell, upper plateau. Terminated.
A-4, Li-Al/FeS_2-CoS_2, U, 0, 115/110, 11.7 × 12.7 × 3.5 cm, 1.2 kg	74	111	9	13	100	80	119	188	23	21	36	23	Upper plateau cell, assembled uncharged. Discharge and cutoff 1.3-2.05 V. Welded Mo sheet current collector. 12-13 mΩ resistance. Hastelloy B frame in positive. Specific energy of 102 W-hr/kg at 14-hr rate and 97 W-hr/kg at 9-hr rate. Terminated, declining capacity.

(contd)

APPENDIX A. Summary of Large-Scale Cell Tests

Cell Description[a]	Max. Performance @ Indicated Rate[b] A-hr	W-hr	Rates, hr Disch.	Charge	Initial Eff.,[c] % A-hr	W-hr	Life Characteristics Days[d]	Cycles[d]	% Decline in[e] Capacity	Energy	A-hr Eff.	W-hr Eff.	Remarks
B7-S, Li-Al/FeS-Cu_2S, C, S, 149/149, 13.5 × 15.6 × 3.8 cm, 3.99 kg	100	246	10	9	99	80	>477	>756	40	57	19	19	Two EP thick electrode cells in series. Total life of 1B4 is 526 days, 789 cycles; 1B6, 499 days, 782 cycles.
	77	176	5	6	99	74							
	57	124	3	4	99	72							
	55	78	1	4	99	70							
B12-S, Li-Al/FeS_2-CoS_2, C, S, 156/143, 13.5 × 15.6 × 3.8 cm, 10.34 kg	81	606	10	10	99	86	23	34	64	67	2	4	Five Eagle-Picher thick electrode cells (I-5-3,4;5,7,8) in series. Equalization charge used.
B13-S, Li-Al/FeS_2-CoS_2, C, S, 156/143, 13.5 × 15.6 × 3.8 cm, 6.24 kg	52	199	3	5	99	72	38	75	-	-	-	-	Three EP thick electrode cells (I-5-4,5,7) in series. No equalization. Tests in Linde insulated case. Terminated.
	45	171	2	4.5	99	69							
	39	140	1.5	4	98	64							

[a] The letters U, C, O, and S are used to indicate uncharged, charged, open, and sealed cells, respectively. The capacity ratio is the number of ampere-hours in the negative electrode over the number of ampere-hours in the positive electrode. In some cases, only the capacity of the limiting electrode is given.

[b] Based on at least five cycles.

[c] Based on at least 10 cycles.

[d] The "greater than" symbols denote continuing operation.

[e] Percent decline from the maximum values at the 5-hr discharge, except where noted.

Distribution of ANL-77-75

Internal:

M. V. Nevitt
R. V. Laney
P. R. Fields
S. A. Davis
B. R. T. Frost
G. T. Garvey
D. C. Price
K. E. Anderson
J. D. Arntzen
J. Barghusen
L. Bartholme
J. E. Battles
E. C. Berrill
C. A. Boquist
L. Burris
F. A. Cafasso
A. A. Chilenskas
K. Choi
P. Cunningham
D. Day
W. DeLuca
R. Dunne
J. G. Eberhart
R. Elliott
W. R. Frost
E. C. Gay
J. Harmon
F. Hornstra
A. A. Jonke
R. W. Kessie
G. M. Kesser
V. M. Kolba
W. Kremsner
M. L. Kyle
W. W. Lark
S. Lawroski
R. F. Malecha
A. E. Martin
F. J. Martino
C. A. Melendres
A. Melton
W. E. Miller
F. Mrazek
K. M. Myles
T. Olszanski
P. A. Nelson (100)
E. G. Pewitt
E. R. Proud
S. Preto
G. Redding
M. F. Roche
L. E. Ross
M. Saboungi
W. W. Schertz
J. L. Settle
H. Shimotake
J. A. Smaga
R. K. Steunenberg
B. Swaroop
C. A. Swoboda
Z. Tomczuk
R. Varma
D. R. Vissers
S. Vogler
W. J. Walsh
D. S. Webster
S. E. Wood
N. P. Yao
P. Eshman
J. E. A. Graae
J. L. Hamilton
P. A. Eident
T. D. Kaun
J. E. Kincinas
K. Kinoshita
Z. Nagy
K. A. Reed
M. A. Slawecki
N. Otto
C. Sy
A. B. Krisciunas
ANL Contract Copy
ANL Libraries (5)
TIS Files (6)

External:

DOE-TIC, for distribution per UC-94c (182)
Chief, Chicago Patent Group
V. Hummel, DOE-CH
President, Argonne Universities Association
Chemical Engineering Division Review Committee:
- R. C. Axtmann, Princeton Univ.
- R. E. Balzhiser, Electric Power Research Institute
- J. T. Banchero, Univ. Notre Dame
- D. L. Douglas, Gould Inc.
- P. W. Gilles, Univ. Kansas
- R. I. Newman, Allied Chemical Corp.
- G. M. Rosenblatt, Pennsylvania State Univ.

J. G. Ahlen, Illinois Legislative Council, Springfield
J. Ambrus, Naval Surface Weapons Center
J. N. Anand, Dow Chemical Co., Walnut Creek, Calif.
F. Anson, California Inst. Technology
P. Auh, Brookhaven National Laboratory
B. S. Baker, Energy Research Corp.
H. Balzan, Tennessee Valley Authority

K. F. Barber, Div. Transportation Energy Conservation, USDOE
H. J. Barger, Jr., U. S. Army MERDC, Fort Belvoir
T. R. Beck, Electrochemical Technology Corp., Seattle
J. A. Belding, Div. Conservation Research & Technology, USDOE
M. Benedict, Massachusetts Institute of Technology
D. N. Bennion, Univ. California, Los Angeles
J. Birk, Electric Power Research Inst.
J. Braunstein, Oak Ridge National Laboratory
M. Breiter, GE Research & Development Center
J. O. Brittain, Northwestern U.
R. Brodd, Parma Technical Center, Union Carbide Corp.
J. J. Brogan, Div. Transportation Energy Conservation, USDOE
E. Brooman, Battelle Memorial Institute, Columbus
B. D. Brummet, McGraw-Edison Co., Bloomfield, NJ
D. M. Bush, Sandia Laboratories
E. Buzzelli, Westinghouse Electric Corp., Pittsburgh
E. J. Cairns, General Motors Research Lab., Warren, Mich.
E. Carr, Eagle-Picher Industries, Joplin
P. Carr, Energy Development Associates, Madison Heights, Mich.
Chloride Systems (U. S. A.) Inc., North Haven, Conn.
C. Christenson, Gould Inc.
C. A. Clemons, PPG Industries, Pittsburgh
M. Cohen, Univ. of Chicago
A. R. Cook, Int'l Lead Zinc Research Organization, Inc., New York City
D. R. Craig, Hooker Chemical Corp.
G. Cramer, Southern California Edison, Rosemead
F. M. Delnick, Sandia Labs.
J. Dunning, General Motors Research Lab., Warren, Mich.
P. Eggers, Battelle Memorial Institute, Columbus
M. Eisenberg, Electrochimica Corp.
R. P. Epple, Div. Physical Research, USDOE
P. L. Fleischner, National Beryllia Corp.
J. H. B. George, Arthur D. Little, Inc.
J. Giner, Tyco Labs., Inc., Waltham, Mass.
G. Goodman, Globe-Union, Inc., Milwaukee
G. Gorten, Gorten and Associates, Sherman Oaks, Calif.
H. Grady, Foote Mineral Co., Exton, Pa.
S. Gratch, Birmingham, Mich.
D. Gregory, Institute of Gas Technology, Chicago
N. Gupta, Ford Motor Co.
N. Hackerman, Rice U.
G. Hagey, Div. of Technology Overview, USDOE
C. Halpin, Halpin Engrs. Grosse Point, Mich.
R. Hamilton, Carborundum Co., Niagara Falls
W. Hassenzahl, Los Alamos Scientific Laboratory
L. A. Heredy, Atomics International
B. Higgins, Eagle-Picher Industries, Joplin
R. Hudson, Eagle-Picher Industries, Joplin
J. R. Huff, U. S. Army Mobility Equipment R&D Center, Fort Belvoir
R. A. Huggins, Stanford U.
R. A. Huse, Public Service Electric & Gas Co., Newark, N.J.
S. D. James, U. S. Naval Surface Weapons Center

M. A. Jansen, Allegheny Power Service Corp., Greensburgh, Pa.
G. Janz, Rensselaer Polytechnic Inst.
H. Jensen, C&D Batteries, Plymouth Meeting, Pa.
F. Kalhammer, Electric Power Research Institute
K. Kinsman, Ford Motor Co.
R. Kirk, Div. of Transportation Energy Conservation, USDOE
K. W. Klunder, Div. of Energy Storage Systems, USDOE
J. Lagowski, Detroit Edison Utility Co.
J. J. Lander, Air Force Aero Propulsion Lab., Wright-Patterson AFB
A. Landgrebe, Div. of Energy Storage Systems, USDOE (6)
C. E. Larson, Bethesda, Md.
S. H. Law, Northeast Utilities, Hartford, Conn.
H. Leribaux, Texas A&M U.
D. Linden, U. S. Army Electronics Command, Fort Monmouth, N.J.
R. Llewellyn, Indiana State U.
P. S. Lykoudis, Purdue Univ.
G. Mamantov, U. Tennessee
J. Mathers, U. Maryland
C. J. Mazac, PPG Industries, Corpus Christi
J. McKeown, Office of Program Administration, USDOE
C. McMurty, Carborundum Co., Niagara Falls
R. McRae, ILC Technology, Sunnyvale, Calif.
D. Meighan, C&D Batteries, Plymouth Meeting, Pa.
R. Minck, Ford Motor Co.
F. Moore, Div. of Energy Storage Systems, USDOE
G. Murray, Detroit Edison Utility Co.
E. Nicholson, Esso Research & Engineering Corporate Res. Lab., Linden, N.J.
C. Pax, Div. Transportation Energy Conservation, USDOE
G. F. Pezdirtz, Div. of Energy Storage Systems, USDOE
R. Rightmire, Standard Oil of Ohio, Cleveland
R. Rizzo, Globe-Union, Inc., Milwaukee
N. Rosenberg, Transportation Systems Center, Cambridge, Mass.
N. W. Rosenblatt, E. I. duPont de Nemours & Co., Wilmington
R. Rubischko, Gould Inc.
A. Salkind, ESB Inc., Yardley, Pa.
G. Scharbach, American Motors General Corp., Wayne, Mich.
T. Schneider, Public Service Electric & Gas Co., Newark, N.J.
R. I. Schoen, National Science Foundation
J. R. Schorr, Battelle Memorial Institute, Columbus
D. R. Schramm, Public Service Electric & Gas Co., Newark, N.J.
H. J. Schwartz, NASA Lewis Research Center
J. R. Selman, Illinois Institute of Technology
A. I. Snow, Atlantic Richfield Co., Harvey, Ill.
S. Srinivasan, Brookhaven National Laboratory
D. Stakem, Catalyst Research Corp., Baltimore
E. Steeve, Commonwealth Edison Co., Chicago
R. H. Strange II, National Science Foundation
R. L. Strombotne, U. S. Dept. Transportation, Washington
S. Sudar, Atomics International
R. H. Swoyer, Pennsylvania Power and Light Co., Allentown
F. Tepper, Catalyst Research Corp., Baltimore
L. Thaller, NASA Lewis Research Center
G. M. Thut, Div. Tranoportation Energy Conservation, USDOE

C. W. Tobias, U. California, Berkeley
L. Topper, National Science Foundation
W. Towle, Globe-Union, Inc., Milwaukee
J. Vanderryn, Office of Intern. R&D Programs, USDOE
J. V. Vinciguerra, Eagle-Picher Industries, Joplin
R. D. Walker, Jr., U. Florida
C. O. Wanvig, Jr., Globe-Union, Inc., Milwaukee
S. A. Weiner, Ford Motor Co.
J. Werth, ESB Inc., Yardley, Pa.
C. Wienlein, Globe-Union, Inc., Milwaukee
F. Will, General Electric R&D Center, Schenectady
J. Withrow, Chrysler Corp., Detroit
W. L. Wonell, U. of California, Berkeley
S. Wood, La Grange Park, Ill.
T. Wydeven, NASA Ames Research Center
O. Zimmerman, Portland General Electric Co., Portland, Ore.
M. Zlotnick, Div. Conservation Research and Technology, USDOE
Chloride Technical Limited, Manchester, England
E. Voss, Varta Batterie A.G., Kelkhern, Germany
E. Aiello, U. of Chicago
W. J. Argersinger, Jr., U. of Kansas
J. T. Banchero, U. of Notre Dame
K. J. Bell, Oklahoma State U.
R. Blanco, Oak Ridge Nat. Lab.
C. F. Bonilla, Columbia U.
W. Brandt, U. of Wisconsin-Milwaukee
A. E. Dukler, U. of Houston
W. J. Frea, Michigan Tech. U.
J. E. Linehan, Marquette U.
Maine Univ., Prof. in charge of Chem. Engr. Lib.
Marquette U., Dept. of Chemistry
Michigan Tech. U., Library
N. R. Miller, United Nuclear Industries, Richland
G. Murphy, Iowa State U.
E. A. Peretti, U. of Notre Dame
C. W. Preckshot, U. of Missouri
H. Rosson, U. of Kansas
C. Sanathanan, U. of Illinois-Chicago Circle
A. Sesonske, Purdue U.
USDOE, Director, Div. of Safeguards and Security
B. W. Wilkinson, Michigan State U.
Comision Nacional de Energia Atomica, Library, Argentina
J. A. Sabato, Com. Nac. de Energia Atomica, Buenos Aires, Argentina
C. H. Cheng, Nat'l Tsing Hau Univ., China
National Radiological Protection Board, Library, Harwell, England
L. Kemmerich, Ges. fur Kernforschung, Karlsruhe, Germany
F. Weigel, Inst. fur Anorganische Chemie der U. Munich, Germany
N. Saratchandran, Bhabha Atomic Research Centre, Bombay, India
K. Fujimiya, U. of Tokyo, Japan
Japan Atomic Energy Research Inst., Tokai-mura, Japan
K. Matsuda, Inst. of Physical & Chemical Res., Yamato-machi, Japan
Sang-Soo Lee, Korea Advanced Institute of Science, Korea
Korean Atomic Energy Research Institute, Korea
Ragnar Nordberg, Sahlgren's Hospital, Goteborg, Sweden

☆ U.S. GOVERNMENT PRINTING OFFICE: 1977—750-133